TÉCNICO LISBOA

Functionalization of Extracellular Vesicles

Rita Leónidas Xavier Esteves Ferreira da Rocha

Thesis to obtain the Master of Science Degree in

Biotechnology

Supervisor: Dr. Fábio Monteiro Fernandes

Co-Supervisor: Dr. Tiago Miguel Peixoto Dias

Examination Committee

Chairperson: Prof. Dr. Arsénio do Carmo Sales Mendes Fialho

Supervisor: Dr. Fábio Monteiro Fernandes

Member of the Committee: Dr. Vasco Daniel Bigas Bonifácio

October 2021

Declaration

I declare that this document is an original work of my own authorship and that it fulfils all the requirements of the Code of Conduct and Good Practices of the Universidade de Lisboa.

Preface

The work presented in this thesis was performed at the Institute for Bioengineering and Biosciences (iBB) of Instituto superior Técnico (Lisbon, Portugal), from September 2020 to October 2021, under the supervision of Dr. Fábio Fernandes and co-supervision of Dr. Tiago Dias.

Acknowledgements

I would like to start by thanking my supervisor, Dr. Fábio Fernandes, for giving me the opportunity to work in and explore such an interesting research topic, and for being available at all times to help me throughout this journey.

I would also like to thank my co-supervisor, Dr. Tiago Dias. There are no words to describe the support I received from him. He was the best teacher, life-guide and friend I could have possible asked for throughout this whole experience. He always kept me motivated and made sure I never stopped believing in myself. For that I am forever grateful. It was a true pleasure to work and learn by his side.

I would like to express my gratitude to iBB for the support and help whenever I needed.

To Raquel Guerreiro, the kindest lab partner. Thank you for you friendship, generosity, for always being there for me and for being such a big part of this experience.

To my best friends, Ana Carolina Malta, Marta Fidalgo and Vitória Cadete. Thank you for your constant support and for being such great examples of true kindness, determination and friendship. I could not be more grateful to have you in my life.

To my family, my parents, and all my 6 siblings. You are part of who I am and I feel this accomplishment is as much mine as it is yours. Thank you for being the best support system anyone could have. The happiness and positivity in which we live every single day is a true inspiration. With you, I feel anything is possible.

Resumo

Os exossomas, uma subpopulação de vesículas extracelulares, estão envolvidos na comunicação intercelular de longa distância e têm um grande potencial como novo sistema de transporte de medicamentos para doenças do Sistema Nervoso Central, como a doença de Alzheimer. A doença de Alzheimer é caracterizada pela deposição do peptídeo β-amilóide como placas amiloides, e um dos potenciais tratamentos para esta doença advém do uso da Neprilisina (NEP), uma enzima degradadora do peptídeo β-amilóide. A fim de aumentar as terapias baseadas nos exossomas, múltiplas modificações podem ser feitas na superfície dos mesmos. Este trabalho tem como objetivo otimizar metodologias para obtenção de exossomas funcionalizados através da fusão com lipossomas sinteticamente funcionalizados. A fusão entre lipossomas não marcados e lipossomas marcados com fluorescência foi realizada através do método de freeze-thaw. Os resultados demostraram que a funcionalização de lipossomas não marcados com características extrínsecas foi alcançada, e mais tarde, a produção de vesículas hibridas, através da fusão com EVs foi também demonstrada. O método de Click chemistry foi utilizado para a bioconjugação de moléculas como o BDP-azide e PEG-azide à superfície dos lipossomas, a fim de mais tarde funcionalizar os EVs. Esta técnica permite a ligação de uma série de diferentes moléculas aos lipossomas, uma vez que qualquer peptídeo conjugado com um grupo azida pode ser ligado aos lipossomas e depois fundido aos EVs. A reação de click chemistry entre os grupos DBCO-PE e o fluoróforo BDP-azide foi extremamente eficiente resultando na ligação quase instantânea de todos os grupos DBCO-PE a moléculas de BDP-azide. A reação de click chemistry com PEG-azide, revelou-se mais lenta. Esta funcionalização foi quantificada para duas concentrações diferentes de DBCO-PE (10 μM e 25 μM). Após 48 h, as eficiências de funcionalização foram respetivamente, 53.85% e 55.17%, sugerindo funcionalização completa do folheto externo dos lipossomas. O potencial impacto negativo da utilização do método de freeze-thaw na atividade da enzima NEP foi também quantificado, demonstrando que a enzima NEP não perde atividade significativa quando sujeita aos diferentes ciclos de freeze-thaw enquanto incorporada na membrana dos EVs. Este resultado favorável sugere que a produção de partículas híbridas EV-lipossoma através da fusão induzida pelo freeze-thaw é um método válido e útil para alcançar a funcionalização das partículas baseadas em EVs.

Palavras-chave:

Vesículas Extracelulares

Exossomas

Lipossomas

Alzheimer

Neprilisina

Engenharia de Exossomas

Click chemistry

Abstract

Exosomes, a subpopulation of extracellular vesicles, are involved in intercellular long-distance communication and have great potential as a new drug delivery system for Central Nervous System diseases like Alzheimer's. The Alzheimer's disease is characterized by the deposition of the β-amyloid peptide as amyloid plaques and one of the potential treatments for this disease could be based on the use of Neprilysin (NEP), a β-amyloid peptide-degrading enzyme. In order to increase the efficacy of current exosome based therapies, multiple surface modifications can be made to exosomes for cellular and subcellular targeting. This work aims to optimize methodologies to obtain functionalized exosomes through fusion with synthetic functionalized liposomes. The fusion between unlabeled liposomes and fluorescent labeled liposomes was performed through the freeze-thaw method. The results demonstrated that the functionalization of unlabeled liposomes with extrinsic characteristics was accomplished, and later, the production of hybrid vesicles through fusion with EVs was also achieved. The Click chemistry method was used for the bioconjugation of molecules such as BDP-azide and PEG-Azide to the surface of liposomes in order to optimize conditions for functionalization of hybrid EV. This technique allows for the attachment of different molecules to the liposomes as any peptide conjugated with an azide group can be bound to liposomes and then fused to EVs. The click chemistry reaction between the DBCO-PE groups and the fluorophore BDP-azide was extremely efficient resulting in the almost instantaneous ligation of all the DBCO-PE groups to BDP-azide molecules. The click chemistry with PEG-azide, revealed to be slower. This functionalization was quantified for two different concentrations of DBCO-PE (10 μM and 25 μM). After 48 h, the functionalization efficiencies were respectively, 53.85% and 55.17%, suggesting complete functionalization of the outer leaflet of the liposomes. The potential negative impact of using the freeze-thaw method on NEP enzyme activity was also quantified, demonstrating that the NEP enzyme does not lose significant activity when subjected to the different freeze-thaw cycles while incorporated into the membrane of the EVs. This favorable result suggests that the production of hybrid EV-liposome particles via freeze-thaw induced fusion is a valid and useful method to achieve functionalization of EVs-based particles.

Keywords:

EVs (Extracellular Vesicles)

Exosomes

Liposomes

Alzheimer

Neprilysin

EV Engineering

Click Chemistry

Table of Contents

List of Tables

List of Figures

Abbreviations

18:1 DBCO PE 1,2-dioleoyl-*sn*-glycero-3-phosphoethanolamine-*N*-dibenzocyclooctyl

AD Alzheimer's Disease

APOE Alipoprotein E

APP Amyloid Precursor Protein

Aβ β-amyloid Peptide

BBB Blood-Brain-Barrier

BDP-azide BODIPY azide

BODIPY Dipyrromethene boron Difluoride

CALLA Acute lymphoblastic leukemia antigen

CHCl3 Chloroform

CNS Central Nervous System

DBCO-CR Dibenzocyclooctyne Carboxyrhodamine

DBCO-PE Dibenzocyclooctyne

DDS Drug Delivery System

DMSO Dimethyl sulfoxide

DNA Deoxyribonucleic Acid

DNAse Deoxyribonuclease

DOPE-cap-biotin Biotinylated phospholipid

DOPE-NBD *N*-(7-Nitrobenzofurazan-4-yl)-1,2-dioleoyl-*sn*-glycero-3-phosphoethanolamine

DOPE-Rho 1,2-dioleoyl-s*n*-glycero-3-phosphoethanolamine-*N*-(lissamine Rhodamine B sulfonyl)

dsDNA Double Stranded DNA

ECE-1 substrate 7-metoxycoumarin-4-yl acetyl (MCA)-Arg-Pro-Pro-Gly-Phe-Ser-Ala-Phe-2,4-dinitrophenyl (DNP)- Lys peptide

EDC Carbodiimide

EOAD Early-Onset Alzheimer's Disease

ESCRT Endosomal Sorting Complex Required for Transport

EtOH Ethanol

EVMs Extracellular Vesicles Mimetics

EVs Extracellular Vesicles

fEOAD Familial Early-Onset Alzheimer's Disease

FRET Förster Resonance Energy Transfer

gRNA Guide RNA

GUV´s Giant unilamellar vesicles

ILV Intraluminal Endosomic Vesicles

lncRNA Long noncoding RNA

LOAD Late-Onset Alzheimer's Disease

MFL Membrane Fusogenic Liposomes

miRNA Micro RNA

mRNA Messenger RNA

MVBs Multivesicular Bodies

NEP Neprilysin

NFL Non Fusogenic Liposomes

NHS N-hydroxysuccinimide

NMDA N-methyl-D-aspartate

NTA Nanoparticle Tracking Analysis

ntDNA Non-target DNA

PBS Phosphate buffered saline

PEG Polyethylene Glycol

PEG-Azide Methoxypolyethylene glycol azide

POPC 1-palmitoyl-2-oleoyl-*sn*-glycero-3-phosphocholine

PSEN1 presenilin 1

PSEN2 presenilin 2

PVA Polyvinyl alcohol

RES Reticuloendothelial System

RNA Ribonucleic Acid

RNAse Ribonuclease

SEC Size-exclusion Chromatography

siRNA Small Interfering RNA

ssDNA Single Stranded Deoxyribonucleic Acid

UV-visible Ultraviolet-visible

I. Introduction

1.1. Extracellular Vesicles

In recent years, intense investigation has been made on membrane trafficking by exosomes, due to their potential as biomarkers for diagnosis and as a route for drug delivery.[1] Exosomes might be an alternative to synthetic nanoparticles, solving clearance problems and preventing toxic effects through a more specific and controlled transport of drugs, particularly important for example in cancer therapeutics or in treating neurological diseases.[2,3]

The process by which macromolecules, as for example proteins, can move throughout a cell or be released into extracellular space is known as membrane trafficking. Extracellular vesicles (EVs), produced by the cell membrane, act as transport intermediaries and can be formed by mechanisms such as endocytosis of clathrine-coated vesicles or direct shedding of the plasma membrane. Extracellular vesicles can be classified by size, content, synthesis, and function and include microvesicles, apoptotic bodies and exosomes.[2,4]

Microvesicle diameter varies between 150 to 1000 nm and they are released from the cell by the outward budding of the plasma membrane, having therefore a similar composition to it. The process through which they are formed is thought to be via shedding directly from plasma membranes.[2] As exosomes, they are cargo transporters and participate in cell–cell communication, and might have clinical applications similar to exossomes in the future.[4,5]

On the other hand, apoptotic bodies are released by dying cells and represent the final consequences of cellular fragmentation. They are 50-5000 nm extracellular vesicles that contain intact organelles, chromatin, DNA, histones and small amounts of glycosylated proteins. They are formed after cell contraction, which results in increased hydrostatic pressure, leading to the separation of the cell's plasma membrane from the cytoskeleton.[2,4]

Exosomes are vesicles of 40 to 150 nm, formed from multivesicular bodies through the inward budding of the endosome membrane, so as microvesicles, they are composed of an aqueous nucleus coated with a lipid bilayer. [4,6] They are involved in intercellular long-distance communication, important for biological processes such as cell proliferation, inflammation, immune response, lactation and neuronal function. They are also involved in the transport, sorting, recycling, storage, transport, and release of lipids, proteins, and nucleic acids.[3,5]

Most cells produce exosomes (as for example platelets, immune cells, hematopoietic cells, epithelial cells, neurons, oligodendrocytes, Schwan cells, tumour cells and adipocytes), and they can be found in many biological fluids (such as blood, urine, semen, breast milk, saliva, amniotic fluid, bile, bronchoalveolar lavage fluid, synovial fluid, and cerebrospinal fluid).[4]

1.1.1. The Origin of Exosomes

Exosomes can originate from two pathways: the classical pathway and the direct pathway. The classical or endocytic pathway has been widely investigated and has three stages. Firstly, an inward budding of the plasma membrane occurs, creating endocytic vesicles (early endosomes that mature into late endosomes). Secondly, multivesicular bodies (MVB) are formed. MVBs are intracellular endosomal organelles, which contain many single outer membrane vesicles, known as intraluminal endosomic vesicles (ILV). They are formed from early endosomes, which are involved in the degradative endosomal pathway of internalized proteins. Thus, some authors recognize two types of MVBs, one in the degradative pathway and another in the exocytosis. Forming MVBs depends on the endosomal sorting complex required for transport (ESCRT). Four complexes, namely ESCRT-0, I, II, III and accessory proteins (Alix, TSG101, HSC70, and HSP90β) act sequentially to bind and sort ubiquitinylated proteins and receptors in the late endosomes. This enables recognition, engagement and concentration of transmembrane proteins, cargo sorting, membrane deformation with bud formation. The third and last step is the vesicle scission, also mediated by the ESCRT complexes (Fig. 1). [2,4]

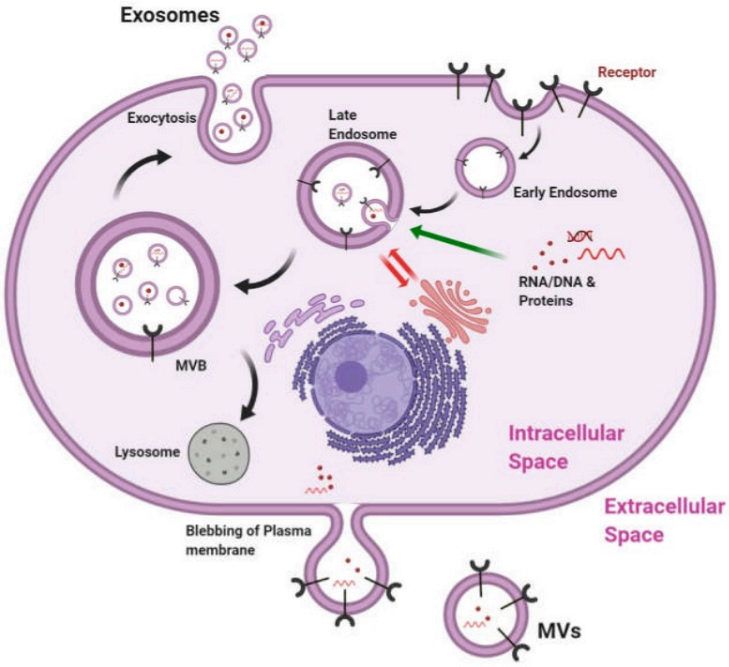

Figure 1 - Biogenesis of exosomes (Adapted from Gangadaran et. al).[7]

There are also ESCRT-independent mechanisms, involving ceramide, tetraspanins or lipopolysaccharide induced TNF factor (SIMPLE), among others. Once MVBs are formed, they can fuse with lysosomes, leading to the degradation of their contents, or with the plasma membrane, releasing the ILVs into the extracellular space, forming the exosome. Some remain attached to the cell surface and some can transport different molecules to nearby or even faraway cells. On the other hand, some

cells, such as the Jurkat T cells release exosomes directly from their plasma membrane, a process called direct pathway. The production of exosomes is stimulated in response to alterations in the microenvironment, such as stimuli or stress factors to which the secreting cell is submitted. The rate of exosome biogenesis is therefore related to the physiological or pathological status of the cell. [2,4]

1.1.2. The Composition of Exosomes

Exosomes from different cell types have different compositions and functions in different biological processes [3] , thus the origin of exosomes is a very important factor in determining their structure, components, functions and potential. [4]

In terms of composition, the main component of exosomes is lipids, such as cholesterol, short-chain saturated fatty acids, waxes and phosphoglycerids.[3] The composition is not exactly the same as the cell membrane of their origin, with relatively less proportion of phosphatidylcholine and diacylglycerol, being enriched in sphingomyelin, gangliosides, and desaturated lipids. The lipid composition varies according to the exosome's origin. [8]

Variety is also present in proteins that have been used as markers to identify and isolate different exosomes. The proteome includes certain groups present in all types of exosomes such as proteins involved in the biogenesis of multivesicular bodies [3], namely endosomal sorting complexes required for transport (ESCRT) proteins, along with the accessory proteins (Alix, TSG101, HSC70, and HSP90β) [4], cytosolic proteins, proteins of thermal shock, tetraspanins (such as CD63, CD9 and CD81) and proteins involved in specific functions, such as transport or intracellular communication mediated by the surface receptors of the target cell. [5,9]

Exosomes produced from the endolysosomal compartment tend to be more enriched in major histocompatibility complex class II (MHC class II) and tetraspanins CD37, CD53, CD63, CD81, and CD82.[8] Polysaccharide and glycan signatures are present on the exosomes' outer surface, predominantly mannose, α-2,3- and α-2,6-sialic acids, complex N-linked glycans, and polylactosamine.[10] Exosomes also carry genetic material, including RNA (mRNA, miRNA, lncRNA, and other RNA species), and DNAs (mtDNA, ssDNA, dsDNA). By transferring miRNA to other cells, they regulate DNA transcription of certain proteins involved in many biological processes. [4,9,10]

1.1.3. Therapeutic Applications of Exosomes

EVs have showed innate therapeutic potential in many areas like regenerative medicine and cancer immunotherapy.[9] They are also involved in certain diseases like diabetes and neurodegenerative processes.[2]

Specifically in the nervous system, exosomes were found to play an important role in tissue repair and regeneration, by helping to promote neuronal survival, myelin formation and neurite growth. On the other hand, pathogenic proteins, such as beta amyloid peptide and superoxide dismutase have been found in exosomes in the central nervous system (CNS) showing the participation of exosomes in disease progression.[4]

As it was said before, EVs have the capacity to perform intercellular communication. For this reason they can be exploited as drug delivery vehicles for the delivery of exogenous therapeutic reagents.[11] EVs can also be used as biomarkers for the diagnostic and prediction of several diseases.[9]

In order to increase the current exosome-based therapies, multiple surface modifications can be made to the exosomes for cellular and subcellular targeting. This can be achieved by combining different technologies, some of which will be discussed in this thesis.

1.1.4. Exosomes as Drug Delivery Systems

As it was mentioned before, exosomes have a very important role in mediating long-distance intercellular communications, being an efficient and economical mechanism of exchanging information among cells. In the past 10 years, researchers have discovered that exosomes play a very important role in controlling normal physiological processes and progression of pathologies like cancer or neurodegenerative processes. Today, therapeutic applications with exosomes are showing promising results in their use for the diagnosis and treatment of cancer, neurological, immunological or infectious diseases, and many others. [3,12]

It is not fully understood by which mechanisms exosomes control functions in cells, but it is known that for it to happen the vesicular content must be transported to the cells and cell interaction with the exosomes must occur. This can be done by 3 different strategies: receptor-ligand interactions, direct fusion of membranes or via endocytosis. The receptor-ligand interaction can cause the fusion of the exosome with the cell membrane and the release of the vesicular cargo or it can also activate a signal transduction triggering a cellular response. The endocytosis strategy is similar to that of receptor-mediated fusion but the difference is that it involves the formation of MVs that can then be delivered via cell fusion.[3]

Exosomes have been used as diagnostic biomarkers and as potential drug delivery vehicles for several years now. Their biocompatibility, no inherent toxicity, stability, low immunogenicity, natural ability to carry intercellular nucleic acids and therapeutics molecules across membranes difficult to cross such as the Blood Brain Barrier (BBB) and adjustable targeting efficiency are just some of the reasons that make exosomes promising drug delivery systems.[12,13] Thus, exosomes provide an enormous potential in the specific and controlled transmission and release of different synthetic and biological molecules in cellular therapy, creating a whole new therapeutic area. [3,12]

1.2. Liposomes

Liposomes are composed of one or more double-layered phospholipid vesicles that enclose an aqueous medium.[14] Their characteristics such as size, lipid composition, charge and preparation method vary greatly.

They have been used in various disciplines such as biophysics, biochemistry and biology and are one of the most used vehicles in drug delivery systems. Their enclosed aqueous phase allow for containment of hydrophilic drugs and their phospholipid bilayer provides an environment for delivery of lipophilic drugs.[15]

They have been used as carriers for all kinds of agents, such as antibiotics, anti-inflammatory drugs, anticancer drugs, genes and several others. The fact that they are biocompatible, non-toxic and biodegradable entities makes them a very attractive tool for the encapsulation of drugs.[16]

The first generation of liposomes were composed of a phospholipid bilayer with anionic, cationic or neutral phospholipids and cholesterol enclosing an aqueous space. One major limitation of these conventional liposomes is their short life span during intravenous circulation due to uptake by the reticuloendothelial system (RES). To overcome this problem, several researchers engineered the surface of liposomes with different substances. One of the methods developed consisted on the conjugation of polyethylene glycol (PEG) to the liposome surface, which resulted in an increase in circulation time and also delayed their clearance from the RES.[14]

The surface modification of liposomes has also been performed with ligands such as small molecules, carbohydrates, polysaccharides, peptides, antibodies and enzymes. These biomolecules work as ligands for the receptors expressed as docking sites on the tissues of interest. The engineering of the surface of liposomes led to an increase in their applications in fields like cancer detection, therapy and drug delivery.[16]

These targeted liposomes exhibit great solubility, higher stability, have specific drug targeting properties, have minimum off-target effects and are required in less quantity when compared to conventional liposomes.[14] These engineered liposomes based on surface modifications are emerging as a valuable pharmacological tool with the ability to overcome the limitations of conventional therapies.[17]

1.3. Alzheimer's Disease

Alzheimer's disease is a chronical disease associated with the progressive damage of neurons and accumulation of misfolded proteins. Clinically, it is characterized by a gradual decline in cognition and changes in behaviour and personality. [18]

It develops very slowly from a pre-clinal stage into fully expressed clinical symptoms. It is the most widespread cause of dementia, and although this disease affects mostly people over 65 years old, there is an AD subtype that can affect younger people, the Early-Onset Alzheimer's Disease (EOAD). The EOAD can occur in two manners: one that shares the same traits as late-onset AD (LOAD) and another that is a consequence of a genetic predisposition, the familial EOAD (fEOAD). Mutations in the amyloid precursor protein (APP), presenilin 1 (PSEN1) and 2 (PSEN2) genes are involved in the majority of cases of fEOAD.[19]

The Alzheimer´s disease is characterized by the deposition of the β-amyloid peptide (Aβ) as amyloid plaques and of the tau protein as neurofibrillary tangles. The development of the neuropathological process is very slow and the asymptomatic stage can last more than two decades. During this stage, it is already possible to observe the accumulation of β-amyloid peptide and tangle formation. This knowledge led to the use of the β-amyloid peptide and tau protein as biomarkers for Alzheimer's disease diagnostics (Fig. 2). [20]

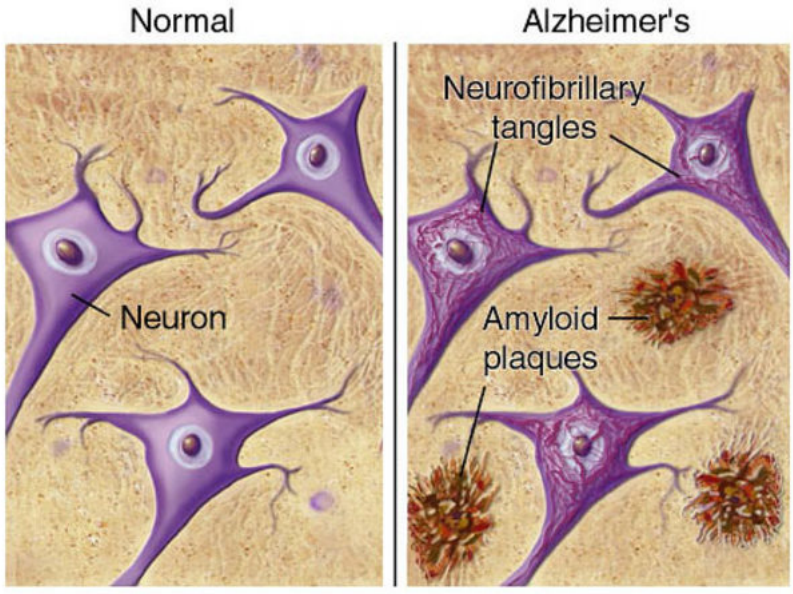

Figure 2 – *Illustration of the comparison between a normal brain and a brain with Alzheimer's disease containing amyloid plaques and neurofibrillary tangles. (Adapted from brightfocus.org)* [21]

In normal conditions, the Aβ peptide is quickly degraded, but sometimes the effectiveness of the metabolic pathway that removes and degrades the Aβ peptide is decreased, leading to the aggregation of the Aβ peptide in oligomers, and then fibrils that ultimately lead to the formation of the

amyloid plaques. For example, people that carry the alipoprotein E (APOE)-ε4 allele are strongly associated with reduced Aβ clearance. The APOE- ε4 isoform is considered to be the strongest genetic risk factor for LOAD.[22] Studies of the preclinical phase of AD have established that APOE- ε4 allele carriers develop enhanced cerebral amyloid deposition with age, and do so at an earlier age, and accumulate amyloid at a more rapid rate when compared to non-carriers.[23]

With the goal of preventing Aβ aggregation, several therapies have been developed. Despite this efforts, currently there is no effective treatment to cure this disease, there are only symptomatic treatments that provide temporary benefit.[24]

In fact, there are only 5 treatments available to treat the symptoms of AD, including four cholinesterase inhibitors and an N-methyl-D-aspartate (NMDA) receptor AD antagonist (memantine). Anti-aggregate drugs such as Tramiprosate and Clioquinol were some of the alternative drugs explored to prevent Aβ aggregation. Unfortunately, these drugs were unable to prevent Aβ aggregation and presented several side effects.[25,20,22,26]

In order to create a disease-modifying treatment for AD, Biogen developed a monoclonal antibody targeting oligomers and fibrils of the (Aβ) protein, named aducanumab. That drug showed to be effective at lowering levels of Aβ. Unfortunately the drug revealed no significant slowing of cognitive decline in patients with mildly symptomatic AD.[27] In a controversial decision, this drug was recently approved by FDA. After a more closely inspection of the data of two phase III clinical trials, Biogen concluded that slowing cognitive decline was statistically significant in a subset of patients.[28] Although, there is not enough data to corroborate the overall efficiency of aducanumab in slowing cognitive decline, this decision brings hope to patients, families and other stakeholders that this treatment can fill the void that, up until now, existed in AD treatment.

All the different treatments mentioned previously showed that an effective therapy for AD has been a major challenge for the pharmaceutical sciences. One of the biggest bottlenecks in brain drug delivery comes from the difficulty of overcoming the BBB. The BBB is an important physical barrier that protects the brain from potential prejudicial substances in the blood circulation. This barrier does not allow the majority of drugs to access the CNS. There have been many innovative attempts to exploit new therapeutic modalities that can overcome the BBB and target drug delivery. The native and unique mechanisms of exosomes confer them great potential as a novel drug delivery system for CNS diseases like AD.[29]

1.3.1 Neprilysin as a potential treatment for Alzheimer's disease

As it was stated before, elevated concentrations of the β-amyloid peptide in the brain play a very important role in the development of Alzheimer's disease. Two possible solutions for slowing down the evolution of AD and lowering brain Aβ levels could be the inhibition of β-amyloid peptide production in the brain or the acceleration of its clearance.[18,30,31]

Neprilysin (NEP), also known as acute lymphoblastic leukemia antigen (CALLA) and CD10, is an integral type II, membrane-bound and zinc dependent endopeptidase. It is considered to be the principal β-amyloid peptide-degrading enzyme in the brain.[18]

NEP becomes inactivated and down-regulated during both the early stages of AD and aging. However, its upregulation leads to the increased degradation of Aβ, therefore reducing the formation of Aβ aggregates and amyloid plaques, preventing pathogenic changes in the brain.[18] Multiple associations of NEP levels with pathology regarding AD have been made, motivating a great interest in manipulating the concentration of this enzyme in the brain.[18] Results suggest that restoring NEP levels in the early stages of AD might be an effective strategy to prevent or mitigate disease progression.[18,31]

1.4. Engineering of EVs

Providing extra-functionality to EVs can enhance their performance, leading to the acceleration of EV-based therapeutics. The engineering of EVs has been mainly done by the manipulation of their internal and external cargo.[32]

For the exosomes to be effectively used as drug delivery systems, therapeutic agents need to be efficiently loaded into the exosomes. There are two approaches that can be followed, the active and passive loading/encapsulation. Passive loading can be achieved by incubation of the exosomes with the drug, where the drug diffuses into the exosome through concentration gradient or by incubation of the drug with the donor cell, where the cells are initially treated with the drug and then the cells secrete the exosomes already with the drug encapsulated. [13]

Active drug loading can be achieved by different techniques such as sonication, extrusion, electroporation, chemical-based exosome incorporation with exogenous cargoes or drug conjugation techniques. This method offers enhanced drug loading efficiency of large molecules. [3,13,33]

In addition, with the purpose of maximizing the therapeutic efficacy and capacity of EVs, extrinsic properties can be provided to them by manipulating their culture conditions.[32] In order to improve the loading efficiency and the targeting of therapeutic molecules towards specific cells, several mechanisms have been developed to functionalize EVs.[34]

Different functionalization strategies can be broadly classified into three major approaches: physical, chemical, and biological engineering methods.[35]

1.4.1. Physical Engineering Methods

The physical engineering of EVs requires minimal manipulation steps and allows the loading of a considerable amount of drugs. It can be done by the passive diffusion of high concentrations of hydrophobic drugs during a simple incubation, where the drug is incubated at a specific temperature for a specific time, followed by purification and isolation.[7] Hydrophobic drugs with significant partition to the hydrophobic membrane can be loaded through this mechanism, while hydrophilic drugs cannot.[32,34]

The encapsulation of hydrophilic molecules (e.g. DNA, RNA) can be achieved by mechanical or chemical disruption of membranes by techniques such as sonication, extrusion, electroporation, freeze-thaw or saponification.[34]

1.4.1.1. Electroporation

Electroporation is a biophysical phenomenon in which brief electrical pulses create transient pores in the membrane, leading to temporary pore formation. Drugs or nucleotides can then enter the EVs.[7] Electroporation can be used to load large molecules, such as nucleic acids (e.g., siRNA, mRNA, and gRNA), and different drugs. Electroporation has a relatively higher drug-loading capacity than incubation, but a lower drug-loading capacity than sonication or saponification. One important drawback of this technique is that it can lead to EV aggregation and deformation.[32,34,36]

1.4.1.2. Sonication

Sonication is another physical treatment to load EVs with hydrophilic drugs. It refers to the process of applying sound energy to agitate particles in a liquid. The mechanical shear force produced by sonication compromises the membrane integrity of EVs, resulting in effective drug loading.[7] It is a widely applicable and simple approach to envelop the drugs with vesicles during the reconstruction of lipids.[34,37] This technique shows an increased drug-loading capacity compared to other methods. It can be used to load various drugs, siRNAs and proteins, but it is unsuitable for hydrophobic drugs.[7]

1.4.1.3. Extrusion

The cell extrusion technique consists in extruding cells through 30–1000 nm pore size membrane filters to break up the cell and then, reform the cell membrane into exosome-mimics (i.e. exosome like vesicles).[34] Extrusion has the highest drug- loading capacity for any kind of drug compared to other methods. On the other hand, it has the disadvantage of creating membrane deformation.

Extrusion is used for the large-scale production of Extracellular Vesicles Mimetics (EVMs) and is also used to produce hybrid EVMs from EVs and liposomes.[7]

1.4.1.4. Saponification

Saponins are naturally occurring, water soluble, surface-active plant glycosides. Saponin has been used to permeabilize the plasma membrane of cells or vesicles to assist cargo loading by inducing the formation of small pores within lipid membranes.[7] The permeabilization of the membrane comes from the binding of saponin to cholesterol and other P-hydroxysteroids present in biological membranes.[38]

Saponin is a toxic agent and because it also gets loaded along with drugs into EVs, additional washing of the EVs is required, which might affect their integrity and process yield. Saponification has a higher drug-loading capacity compared to mixing or simple incubation.[7]

1.4.1.5. Liposome Fusion

This method allows the modification of the exosomal membrane by fusion with liposomes containing peptides, antibodies, polyethylene glycol (PEG) and other molecules capable of improving the delivery functionality of exosomes, targeting of specific cells, protection against immunological system, and many others.[34]

The freeze-thaw method, performed for liposome fusion, is a straightforward technique used to load drugs into EVs. EVs are mixed with drugs, and then they undergo a few cycles of freezing at -80 °C in liquid nitrogen and thawing at room temperature.[7]

The freeze-thaw method briefly disrupts the vesicle membrane by the temporary formation of ice crystals, thereby causing mechanical disruption of the membrane, enabling the loading of EVs and their mimetics with functional biomolecules.[32,35] This process has a relatively moderate drug-loading capacity.[7]

Studies have showed that the method of liposome fusion has efficiency advantages over loading exogenous agents directly to isolated EVs by electroporation or co-incubation, and genetic engineering of parental cells to produce modified EVs. In addition, aggregation and damage to EVs that might occur during the previously mentioned methods for EV engineering can be minimized by this method.[39]

The freeze-thaw method is also used for making hybrid EVMs from EVs and liposomes. In this case, the fusion process can be monitored by Förster resonance energy transfer (FRET).[7,35] The fusion

of functionalized liposomes with EVs combines the advantages of liposomes technology and the natural features of EVs, enabling the efficient loading of therapeutics to EVs.[40,41]

Sato *et al*. has reported functionalization of the surface of EVs by hybridizing it with PEGylated liposomes using freeze-thaw facilitated membrane fusion (Fig. 3).[35,42]

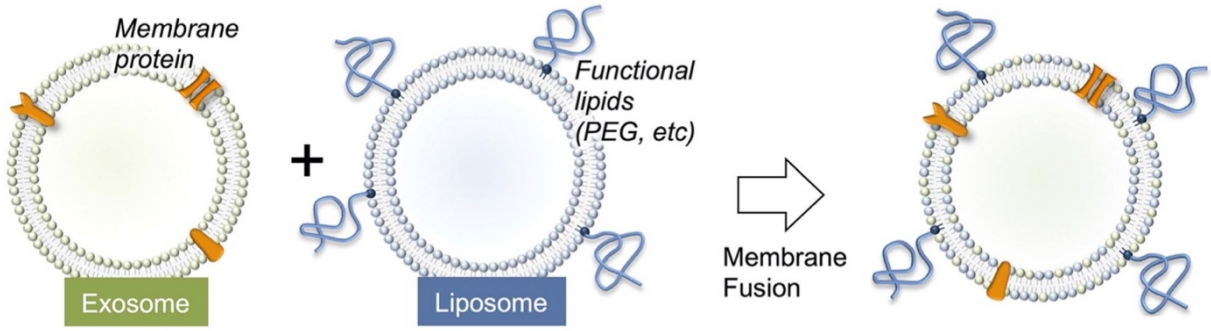

Figure 3 - Schematic of the method used to engineer the exosome-liposome hybrids (Adapted from Sato et. al). [39]

As an alternative to freeze-thaw, Piffoux *et al*. proposed the polyethylene glycol (PEG) – induced fusion of liposomes of known composition with EVs to create hybrid EVs, that can later be used as a personalized DDS.[41] The results highlighted that PEG can induce the fusion between EVs of different cell origins and liposomes of various compositions, and that in optimized conditions, more than 60% of membrane and soluble contents of liposomes could be transferred to EVs, confirming an effective functionalization.[41]

This strategy can be applied to load EVs from different cellular origins with almost any compound associated with synthetic liposomes. Hydrophilic compounds such as siRNA, miRNA, chemotherapeutics agents and others can be encapsulated in the liposome inner core, while lipophilic compounds such as membrane proteins, PEGylated lipids or targeting agents can be located in the liposome bilayer surface. [41] In this specific case, MSC-derived EVs were fused with PEGylated liposomes, allowing a lower internalization by macrophages. These hybrid EVs have also showed to be more effective in delivering antitumor drugs to tumour cells when compared to their precursor liposomes. [41]

Another example of this method is reported by Lee *et al*. where the researchers fused liposomes containing florescent and azide lipids with cancer cell lines by co-incubation, followed by isolation of the exosomes from the medium, resulting in exosomes with a modified membrane containing the phospholipids embedded in fusogenic liposomes.[39]

1.4.2. Biological Engineering Methods

The biological approach for surface functionalization of EVs is achieved by genetically engineering the parental cells into expressing the proteins or cargo of interest, giving rise to the formation of EVs with pre-programmed cargo.[32] This can be made by exploiting the cellular machinery of EVs biogenesis. [35]

Normally, in this technique, cells are transfected with miRNA or target/therapeutic protein-coded plasmids. These genes/proteins are then expressed in the cell and will be present in secreted EVs. [35]

This method can be very beneficial, because it allows for the loading of drugs to EVs without compromising their overall integrity. On the other hand, the heterogeneity in secreted EVs populations and their difficult purification represent major challenges in this biological method. [35]

The functionalization of EVs by the engineering of parental cells can be achieved with techniques such as transfection, modulation of the EV machinery, light irradiation and fusogenic liposome - based modifications.[32]

1.4.2.1. Loading of Cells with Functionalized Membrane Fusogenic Liposomes

Although genetic modification of parental cells is an efficient method for loading drugs to EVs, their cargo is limited to genetic or translational biomolecules.[32] As stated earlier, the functionalization of EVs by the engineering of parental cells can also be made by fusogenic liposome - based modifications. Liposomes are flexibly drug delivery systems that can be surface-modified with various molecules [16] , loaded with both hydrophilic and hydrophobic payloads and are easy to functionalize.

The fusogenic liposomes allow the transport of drugs to both cytosolic and membranous regions of the parental cells. The subsequent handover of the drug-enriched EVs to adjacent cells through the fusogenic liposome based approach has proven to be very advantageous.[32]

This method allows the EVs to be equipped with various functional agents, including fluorophores, lipids, drugs, and bio-orthogonal chemicals without modification of the native lipids and proteins.[39]

Lee *et al*. performed an experience using membrane fusogenic liposomes (MFL) to deliver lipophilic and hydrophilic agents into the cellular membrane and cytosol, respectively, by fusion of the liposomal and plasma membranes.[39] Researchers evaluated the subcellular distribution of lipophilic and hydrophilic cargoes delivered via synthetic liposomes and their subsequent encapsulation into EVs. The final results suggested that the lipophilic and hydrophilic compounds were efficiently co-packaged into the secreted EVs when delivered to parental cells via MFLs and that this method was more efficient

than using NFL (non-fusogenic liposomes) that presumably entrapped both cargos into early endosomes.[39]

They also tested the incorporation of lipids into EVs. They used MFLs to selectively deliver fluorescent phospholipids to the parental cell plasma membrane, leading to the loading of the phospholipids into the EVs membrane. They confirmed the incorporation of the fluorescent phospholipids into the EVs by measuring the fluorescence of the EVs secreted from the cells.

1.4.3. Chemical Engineering Method

Chemical methods can also be used to attach molecules directly to the surface of exosomes via covalent bonds leading to the functionalization of the exosomes. Click chemistry or Copper-catalysed alkyne cycloaddition is an ideal technique for the bioconjugation of small and macro-molecules such as nucleic acids, lipids and proteins to the surface of exosomes.[37] The conjugation of these targeting ligands to the exosome surface may enable specific interactions of exosomes with target cells. Click chemistry is characterized for being a fast and simple technique with high specificity and high yield.[43]

Click chemistry is described as the reaction between an alkyne chemical group and an azide chemical group to form a triazole linkage.[37] This reaction can occur with or without a copper catalyst. The copper-free click chemistry could be beneficial for in vivo application of the engineered EVs, since the copper-catalysed approach may cause cytotoxicity.[32,43]

Click chemistry can be performed under physiological conditions and the reaction's resulting chemical bonds are irreversible.[43] One other advantage of using click chemistry with biomacromolecules is that there are rarely any nonaromatic double bounds that could lead to unwanted side reactions. [44]

Click chemistry can affect not only the biodistribution of exosomes but can also be used as an efficient tool for the labelling of exosomes with fluorescent or radioactive agents for the precise tracking of injected exosomes.[44]

Because the surface functionalization of the EVs with click chemistry is made after the production of the EVs, the purification and separation steps to isolate the functionalized EVs is much simpler in this method when compared to the physical or biological methods.[35]

There are different chemical strategies that can be used to functionalize EVs surface, one of them, the copper-catalyzed azide-alkyne cycloaddition was described by Smyth and colleagues. This technique was used to directly functionalize EVs surface with azide functionality.[44]

First of all, the researchers conjugated a terminal alkyne group to the EVs using EDC/NHS coupling chemistry. Following this functionalization, the EVs were conjugated with Azide-Fluor 545 using

copper-catalyzed azide-alkyne cycloaddition (Fig. 4). The effectiveness of the functionalization was quantified spectrophotometrically by measuring the fluorescence of Azide-Fluor 545. The authors reported that the proposed method of surface functionalization had little to no impact on EVs size and internalization behaviour.[44]

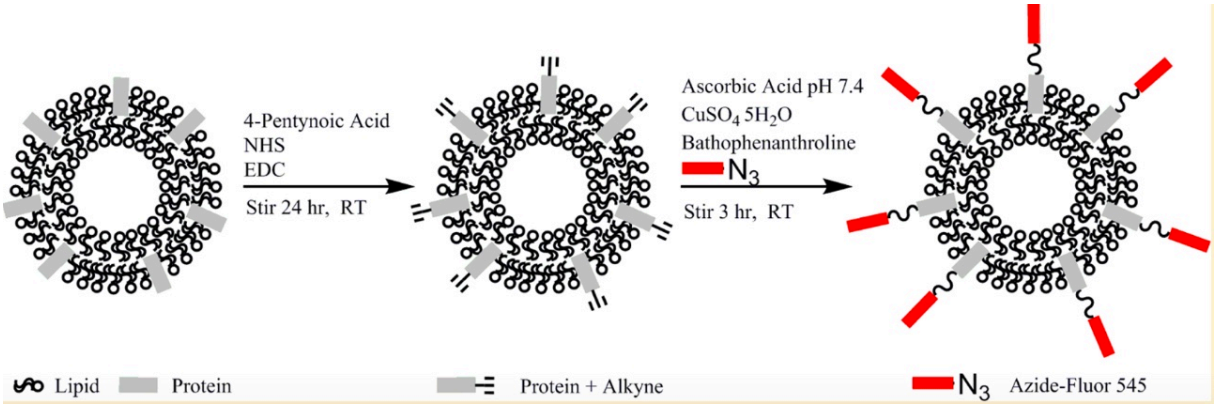

Figure 4 - Modification of exosomal amine groups with a terminal alkyne, followed by conjugation of azide-fluor 545 to exosomes using click chemistry (Adapted from Smyth et. al).[44]

Another chemical strategy used to functionalize EVs was elaborated by Lee and colleagues.[39] The main purpose of this experiment was to perform cellular engineering with membrane fusogenic liposomes to produce functionalized EVs. In order to functionalize the liposomes surface membrane they used copper-free click chemistry.[39]

The method employed is based in the rapid and selective reaction of dibenzocyclooctyne (DBCO-PE) groups with azides to form a stable triazole in physiological conditions. Results revealed that the cells treated with MFLs containing azide-lipids followed by treatment of DBCO-carboxyrhodamine (DBCO-CR) presented CR fluorescence mainly on the plasma membrane, indicating the efficient incorporation of azide-lipids into the plasma membrane.[39] The EVs produced from the cells treated with azide-MFL also showed considerable marked fluorescent when reacted with DBCO-CR directly.[39]

With this experiment authors concluded that through liposome-based cellular engineering, EVs containing azide-lipids could be prepared and easily decorated with various functional ligands by using copper-free click chemistry.[39]

Depending on the type of cells that produce and receive the EVs, delivery efficiencies of the cargo via EVs can differ greatly. In cases where delivery is not sufficiently effective, the surface functionalization of EVs with targeting ligands can promote delivery by concentrating EVs in the surface of target cells.

II. Materials and Methods

2.1. Materials

2.1.1. Chemical Reagents.

1-palmitoyil-2-oleoyl-*sn*-glicero-3-phosphocholine (POPC) and 1,2-dioleoyl-*sn*-glycero-3-phosphoethanolamine-*N*-dibenzocyclooctyl (DBCO PE) were purchased from Avanti Polar Lipids (Alabaster, AL, USA). Phosphate buffered saline (PBS) was purchased from Thermo Fisher Scientific, ethanol (EtOH) and chloroform ($CHCL_3$) were purchased from JMGS. Methoxypolyethylene glycol azide (PEG-Azide), Dimethyl sulfoxide (DMSO) was purchased from Sigma-Aldrich. Milli-Q water was used throughout the work.

2.1.2. Probes.

1,2-dioleoyl-s*n*-glycero-3-phosphoethanolamine-*N*-(lissamine Rhodamine B sulfonyl) (DOPE-Rho) and *N*-(7-Nitrobenzofurazan-4-yl)-1,2-dioleoyl-*sn*-glycero-3-phosphoethanolamine (DOPE-NBD) were both purchased from Avanti Polar Lipids. BODIPY FL azide (BDP-azide) was purchased from Lumiprobe.

2.1.3. Peptides and Enzymes.

ECE-1 substrate - 7-metoxycoumarin-4-yl acetyl (MCA)-Arg-Pro-Pro-Gly-Phe-Ser-Ala-Phe-2,4-dinitrophenyl (DNP)- Lys peptide (ECE-1 substrate) was purchased from Sigma-Aldrich. This peptide has a molecular weight of 1388 g/mol**.** To prepare aliquots of this peptide, the solution was reconstituted in DMSO, originating sample stocks with a concentration of approximately 4 mM. Aliquots were stored at -20 ºC.

Neprilysin - Purified Neprilysin from porcine kidney was purchased from Sigma Aldrich. The enzyme was reconstituted using PBS. Aliquots were stored at -20 ºC with a concentration of 500 nM.

DNA constructs - *pCMV3-MME-OFPSpark and pCMV3-MME*

Human CD10/MME ORF mammalian expression plasmid was purchased from Sino Biological. This vector expresses NEP in its host cells and has a size of 6806bp. In the *pCMV3-MME-OFPSpark*, a C terminal OFPSpark (fluorescent protein) is fused to the expressed NEP. The vector is expressed in mammalian cells. Using T7(TAATACGACTCACTATAGGG) as the forward prime and BGH(TAGAAGGCACAGTCGAGG) as the reverse prime, it was possible to sequence the plasmid.

2.2. Methods

2.2.1. Liposome preparation

For the execution of the FRET assays, the liposomes were prepared using POPC and fluorescently labeled lipids (DOPE-NBD and DOPE-Rho). Samples were prepared with 100% POPC, POPC:DOPE-NBD 99:1, and POPC:DOPE-NBD:DOPE-Rho 98:1:1 mol:mol:mol. For the functionalization of EVs with liposomes, the liposomes were prepared using POPC and DBCO-PE. The different concentrations of DBCO-PE used throughout this project are detailed in the results section for each experiment. After mixing in eppendorfs, the solvent from the different lipid stock solutions was evaporated under nitrogen gas flow. The eppendorf's were then left in vacuum overnight for removal of solvent traces. The next day, 1 ml of PBS (heated at approx. 70 degrees Celsius) was added to each eppendorf for hydration of lipid films and the solutions were vortexed. Afterwards, the freeze-thaw cycles were performed and all samples were frozen in liquid nitrogen at -196 ºC, subsequently fully heated up to 70 ºC and then vortexed. This process was repeated for 8 cycles. The next method employed was extrusion. Extrusion is a technique where the liposome suspension is passed through a membrane filter of defined pore size.[45] All three samples were extruded through a polycarbonate membrane filter with 100-nm pores purchased from Whatman. Filter supports with 10 mm from Avanti Polar Lipids were also used in this technique. First of all, all membranes were hydrated with PBS, then the extruder was assembled and PBS was passed through the system before any other solution did. POPC, POPC plus DOPE-NBD, POPC plus DOPE-NBD, DOPE-Rho and POPC plus DBCO-PE were extruded 21 times.

2.2.2. Membrane Fusion

The POPC liposomes without fluorescent labeled lipids were fused with liposomes with DOPE-NBD or with liposomes with DOPE-NBD and DOPE-Rho. The fusion of the membranes of the different liposomes was established using the freeze-thaw method. As mentioned earlier, this method implies that the solutions are frozen in liquid nitrogen at about −196 °C and then are thawed at 70 ºC and vortexed after each cycle. For the optimization of the fusion process, different ratios and different number of freeze-thaw cycles were tested. With each ratio, samples would go through 2 ,4 and 8 cycles of freeze-thaw.

2.2.3. Fluorescence measurements

The fusion efficiency was evaluated using FRET assays. NBD and rhodamine are an excellent FRET pair and FRET efficiencies can be quantified through measurements of NBD fluorescence intensity. The sample's fluorescence was measured using a FP-8500 fluorescence spectrometer (JASCO, Tokyo, Japan). Fluorescence emission spectra of all samples were obtained with excitation of

DOPE-NBD at 460 nm. For POPC:DOPE-NBD 99:1 mol:mol samples, a single fluorescence peak is detected at ~ 530 nm, corresponding to the NBD fluorescence. For POPC:DOPE-NBD:DOPE-Rho 98:1:1 mol:mol:mol samples, two peaks are observed, at 530 and 580 nm, corresponding to the emissions from DOPE-NBD and DOPE-Rho, respectively. Dilution of DOPE-Rho due to membrane fusion with "empty" liposomes increases the fluorescence intensity at 530 nm and decreases the intensity at 580 nm, as result of lowering FRET efficiencies. The FRET efficiency of the different liposome mixtures was defined as:

$$E = 1 - (I_{DA}/I_D) \qquad \textbf{Eq. 1}$$

where I_{DA} corresponds to the NBD fluorescence intensity of the liposomes marked with both DOPE-NBD and DOPE-Rho, and I_D corresponds to the NBD fluorescence intensity of the liposomes marked with DOPE-NBD. NBD fluorescence intensity was calculated by integrating the signal from 470 to 530 nm, which excludes the signal from rhodamine. The measurements in the fluorescence spectrometer were carried out using 0,5 cm x 0,5 cm width quartz cuvettes at room temperature.

2.2.4. Confocal fluorescence microscopy

Confocal laser scanning fluorescence microscopy measurements were performed on a Leica TCS SP5 (Leica Microsystems CMS GmbH, Manheim, Germany) inverted confocal microscope (DMI600). A 63x apochromatic water immersion objective with a NA 1.2 (Zeiss, Jena Germany) was used for all measurements. Excitation lines were provided by an argon laser. GUVs formulated containing DOPE-Rho and detection of conjugation with BDP-azide was achieved by using an excitation line of 476 nm with detection between 490 - 530 nm for BDP-azide and an excitation line of 514 nm with detection between 550 - 700 nm for DOPE-Rho. All analysis of confocal imaging data was carried out using *ImageJ*.

2.2.5. Absorption measurements

UV-visible absorption spectroscopy measurements were achieved at room temperature using a double beam V- 660 Jasco spectrophotometer (Jasco Corp., Tokyo, Japan). To determine probe and peptide concentrations, the absorption spectra were measured in a 1 cm x 1 cm or 0.5 cm x 0.5 cm path length quartz cuvettes (Hellma Analytics) using a bandwidth and sampling interval of 1 nm.

2.2.6. Nanoparticle Tracking Analysis (NTA)

Nanoparticle Tracking Analysis was used to obtain the concentration and size of particles present in the samples. This technique has been used to characterize vesicle dimensions and uses laser light scattering microscopy and the Brownian motion properties to measure the size of the particles. NTA measurements were carried out on a Nano Sight LM14c instrument equipped with a 405 nm laser (Malvern) and NTA software version 3.1 (Malvern). NTA acquisition and post-acquisition settings were optimized and kept constant for all samples. These settings were established using silica 100 nm microspheres (Polysciences, Inc.)[46] and subsequently adjusted for optimal detection of liposomes and EVs. The liposome samples were diluted in 1.5 mL of PBS 1x in UltraPureTM DNase/RNase-Free distilled water (Thermo Fisher Scientific), to obtain a final concentration in the range of 0.5-3 x 10^9 particles/mL. Acquisition temperature was controlled and maintained at 20 ºC. Each sample was recorded 5 times for 30 s, using fresh sample for each acquisition. The detection chamber was thoroughly washed with PBS between each sample measurement. A threshold level of 7 was applied for video processing. Each video recording was analysed to obtain the size and concentration of the liposomes.[46,47]

2.2.7. Click Chemistry

The reaction of click chemistry in liposomes was carried out with different ligand concentration and the reaction was monitored at different reaction times, in order to identify optimum reaction conditions. Firstly, the reaction was performed using liposomes labeled with DBCO-PE reacting with BDP-azide, to study the effectiveness of the incorporation of azide-lipids into the membrane of the liposomes. UV-visible absorption spectroscopy measurements were taken right after the addition of the BDP-azide and then at 3 h, 6 h, 24 h and 48 h after the beginning of the reaction, depending on the experiment. The samples were kept in constant stirring for the whole reaction process. Later in this project, this same method was used to functionalize liposomes with DBCO-PE, using a different chemical compound PEG-azide. The Reaction was performed in the same conditions as described previously. The different concentrations of DBCO-PE, BDP-azide and PEG-azide used throughout this project are detailed in the results section for each experiment.

2.2.8. Purification with Centrifugal Filter Units

After the click chemistry reaction, in order to purify the samples from any undesired compound, the filtering units Vivaspin® 500 Polyethersulfone, 300 kDa from Sartorius were used. First a coating of the filter unit was made using a buffer of BSA in PBS. The filter unit was centrifuged for 3 minutes and then the buffer was removed. The sample was then added to the filter unit and centrifuged for 30 seconds at 1200 G. After centrifugation the samples were recovered to eppendorfs and the same

amount of flowthrough removed from the filter unit was added as PBS buffer. This process was repeated 4 times giving a total of 5 fraction of sequentially purified samples.

2.2.9. Purification with Size-exclusion Chromatography

Another purification method studied was the Size-exclusion Chromatography (SEC). The main principle of this technique is the adsorption of the solutes of a solution with the help of a stationary phase and afterwards, the separation of the initial solution into independent compounds. First of all, the column was washed 4 times with 5 mL of PBS buffer (mobile phase) and only then was the sample introduced to the column. After the introduction of the sample in the column, a total volume of 7.5 mL of PBS was used to elute the sample and 15 different fractions with volumes of 0.5 mL were recovered and the purification of the sample was achieved.

2.2.10. Formation of Giant Unilamellar Vesicles (GUV´s)

GUVs are a model membrane system comprised of a lipid bilayer with a diameter larger than 1 μm, which can be obtained by gel-assisted formation. The lipid mixture used was composed of POPC (1500 μM), DOPE-Rho (15 μM) and DBCO-PE (25 μM). A solution of 5% (w/w) polyvinyl alcohol (PVA) MW ~145 000 and 280 mM of sucrose was spread in a μ-slide chamber from Ibidi (Munich, Germany) and left to dry for 15 minutes at 50 ºC. The desired lipid mixture was then spread on the PVA surface. The solvent was evaporated for 15 minutes under vacuum. After evaporation of the solvent, the appropriate buffer solution (PBS buffer) was added, allowing for GUV formation for 60 minutes at room temperature. After the formation, GUVs were transferred to a μ-slide chamber with the appropriate coating.

For the immobilization of GUVs in the coverslip surface for imaging in the confocal fluorescence microscope, a small concentration of biotinylated phospholipid (DOPE-cap-biotin) was added to the lipid mixture. Slides from Ibidi (Munich, Germany) were coated with avidin by incubation for 1 hour with 200 μL of a concentrated (0.5mg/ml) solution of the protein, followed by extensive rinsing with MilliQ water and sample buffer. Sucrose containing GUV solutions were transferred to these slides and the glucose solution was then added to the vesicles in order to create a density difference and promote sedimentation of vesicles in the bottom coverslip so that a greater number of vesicles could be imaged. Before any measurements, the slides were left immobile in the dark during 20 min, allowing for the GUVs to attach to the surface.

2.2.11. Extracellular Vesicles Isolation and Quantification

EVs were isolated from conditioned medium collected after 48 hours using the Total Exosome Isolation commercial kit (Invitrogen). Cells were seeded at a density of 6 x 10^6 per cm^2 and transfected with pCMV3-MME-OFPSpark plasmid using Transporter 5™ as a transfection reagent. Cells were maintained for 48 h in a T75, in DMEM supplemented with 10% Exosome-depleted FBS and 1% PenStrep at the incubator with controlled temperature (37 ºC) and humidity and CO_2 levels (5%). After 48h, conditioned medium containing EVs was collected and centrifuged for 30 min at 2000xg to remove cells and cellular debris in suspension. Subsequently, supernatant (~14 ml) was transferred to a falcon and mixed with ~7 ml of Total Exosome Isolation solution and stored overnight at 4 ºC. In the next morning, the mixture was centrifuged at 10000 x g for 1 h (4 ºC). Finally, the pellet containing the EVs was carefully resuspended in PBS to obtain a concentration factor of 40. EV samples were stored at -80 ºC.

The approximate concentration of Neprilysin-OFPSpark in the samples was obtained using a spectrofluorometer (HORIBA) using a OFPSpark calibration curve. Fluorescence measurements of OFPSpark were made with excitation at 535 nm.

2.2.12. Activity assays with ECE1-substrate

The activity of the NEP enzyme when subjected to various freeze-thaw cycles was tested by performing activity assays with ECE-1-substrate. Activity assays with ECE1-substrate were carried out at 37ºC in the microplate reader using the following filters: excitation: 320/10 nm; emission: 370/10 nm.

For this assay, four solutions of NEP with PBS buffer were subjected to freeze-thaw cycles (0,2,4 and 8 cycles respectively). The conditions in which this technique was performed were the same as the ones described previously for the freeze-thaw method. After the cycles, NEP was added to 10 µM solutions of ECE1-substrate. Measurements were carried out with 3 replicates for each condition. The samples were added to the microplate right before initiating the measurements.

For activity assays using the EVs, measurements were also carried out at 37ºC. EVs loaded with NEP-OFPSpark had a concentration of 4.35 x 10^{10} particles/mL and were diluted to a final concentration of 0.1 nM of OFPSpark. Naive EVs, without NEP-OFPSpark, had a particle concentration of 8.25 x 10^{10} particles/mL.

III. Results and Discussion

3.1. Fusion between unlabeled liposomes and fluorescent labeled liposomes

Before testing the efficiency of the EV-liposome fusion, the fusion between unlabeled liposomes and fluorescent labeled liposomes was performed. Unlabeled liposomes were fused with fluorescent labeled liposomes by the freeze-thaw method. The fluorescently labeled liposomes were prepared by freeze-thawing and extruding an aqueous liposome dispersion comprising POPC and fluorescently-labeled lipids, DOPE-Rho and DOPE-NBD. The set of NBD and Rho-labeled lipid, very commonly used for the analysis of liposome-liposome fusion, were used to evaluate the efficiency of the liposome fusion in terms of lipid mixing ratio, measured using Förster-resonance energy transfer (FRET). The concentration of NBD and Rho-labeled lipids within the liposomes was consistently 1:100 (molar ratio) of total lipid.

The NTA revealed that the hydrodynamic diameter of the liposomes labeled with NBD was 168.5 ± 2.5 nm (mean ± standard deviation) and for the liposomes labeled with NBD and Rho, was 169.9 ± 5.2 nm (mean ± standard deviation) (Fig. 5).

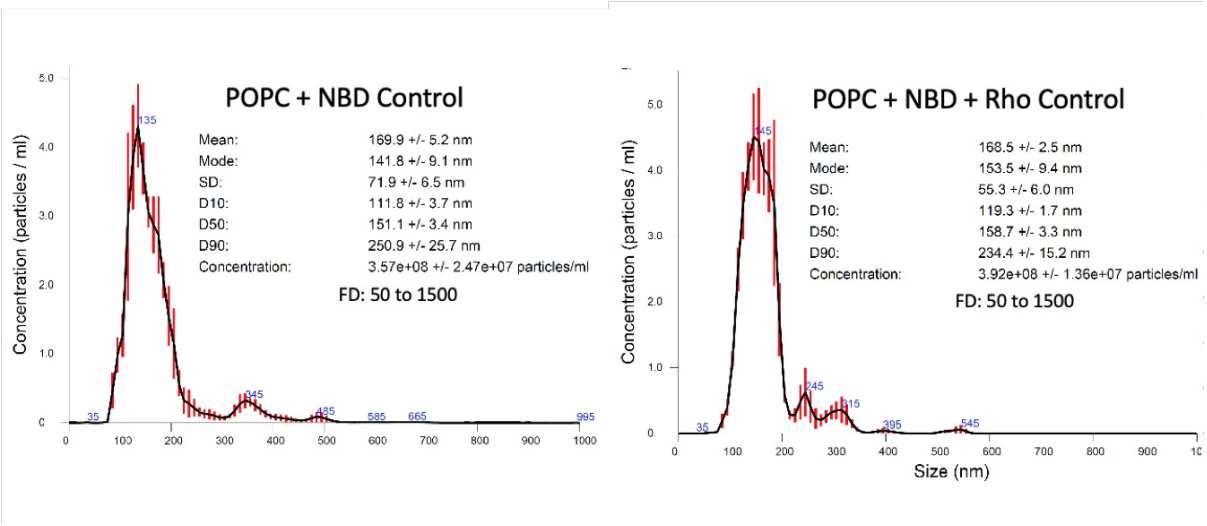

Figure 5 - Size distribution profile, as determined by nanoparticle tracking analysis.

The labeled liposomes were mixed with the unlabeled liposomes at volumetric ratios of 1:1, 1:2, 1:5 and 1:10. Liposomes were diluted to a concentration of 5 μM (total lipid), corresponding to a concentration of 0.05 μM of NBD/Rho. To induce membrane fusion, mixtures were frozen in liquid nitrogen at -196 ºC and thawed at 70 ºC.

The results from the fusion of unlabeled liposomes with NBD-labeled liposomes showed that the intensity of fluorescence of the FRET donor exhibited only minor changes with further cycles of freeze-thaw for all 4 ratios of labeled to “empty” liposomes. This was expected, as the concentration of NBD labeled lipids is not sufficient to achieve significant self-quenching. If it was, this would be alleviated upon events of fusion with “empty” liposomes, and donor fluorescence would increase with further membrane dilution (Fig.6).

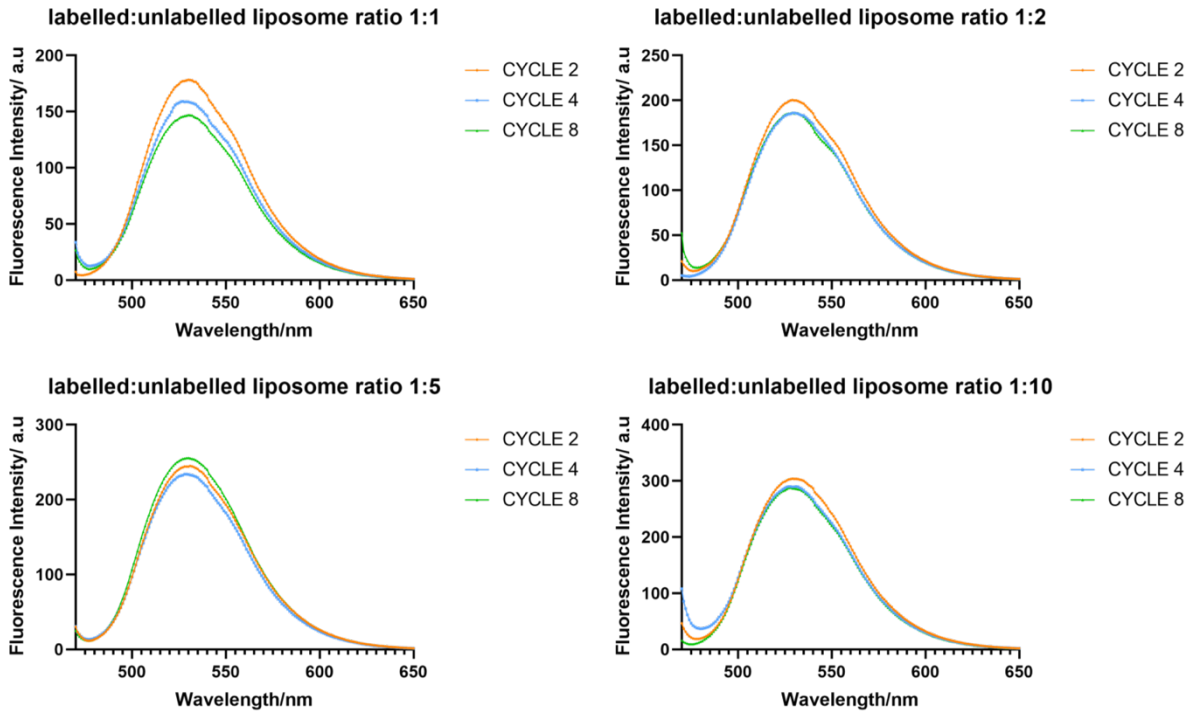

Figure 6 – Fluorescence emission spectra of NBD-labeled liposomes after fusion with unlabeled liposomes at four different ratios of labeled to "empty" vesicles (1:1, 1:2, 1:5, 1:10). The orange line corresponds to the cycle 2 (2 rounds of freeze-thaw), the blue line corresponds to the cycle 4 (4 rounds of freeze-thaw) and the green line corresponds to the cycle 8 (8 rounds of freeze-thaw).

Fusion of "empty" liposomes with liposomes labeled with both DOPE-NBD and DOPE-Rho (at the same concentrations as used above for DOPE-NBD only liposomes) was performed (Fig.7), and it was observed that when DOPE-NBD is excited at a wavelength of 460 nm, the resulting solutions present fluorescence spectra with peaks at 530 and 580 nm, reflecting the emission from DOPE-NBD and DOPE-Rho respectively. After subjecting the labeled-liposome/"empty" liposome mixture to freeze-thaw cycles, the fluorescence intensity at 530 nm increases and the intensity at 580 nm decreases as the number of cycles increase. The results are consistent for all the different ratios, and reflect the dilution of donors and acceptors in the membrane due to fusion with unlabeled liposomes (Fig.7). This dilution increases the average distance between donors and acceptors, decreasing FRET efficiency.

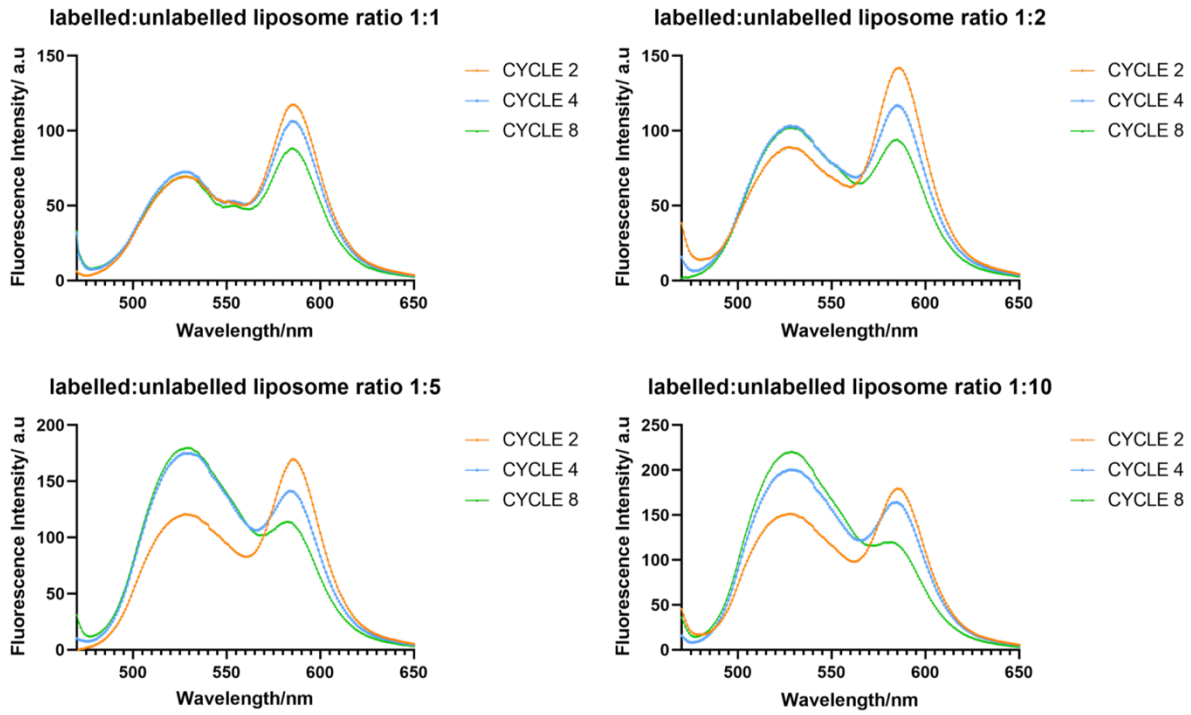

Figure 7 – Fluorescence emission spectra of NBD- and Rho-labeled liposomes after fusion with unlabeled liposomes at four different ratios of labeled to "empty" vesicles (1:1, 1:2, 1:5, 1:10). The orange line corresponds to the cycle 2 (2 rounds of freeze-thaw), the blue line corresponds to the cycle 4 (4 rounds of freeze-thaw) and the green line corresponds to the cycle 8 (8 rounds of freeze-thaw).

A total of 4 replicates (n=4) were executed and the results are illustrated in Fig.8 as a measure of FRET efficiency. FRET efficiency values are shown relative to the ratio of labeled to unlabeled liposomes and number of freeze-thaw cycles.

The FRET efficiency of the different liposome mixtures was defined as $E=1-(I_{DA}/I_D)$, as described before.

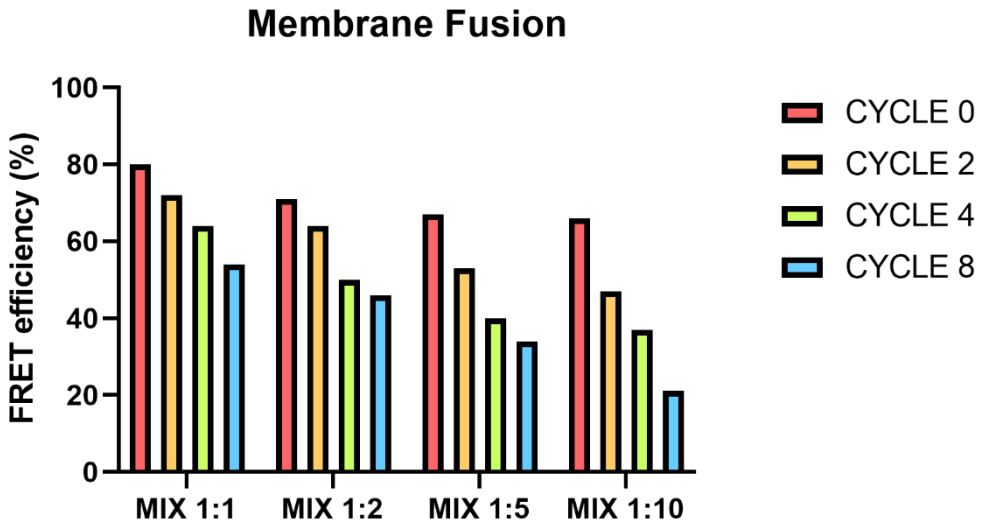

Figure 8 - FRET efficiency of the different liposome mixtures was defined as E= 1 - (I_{DA}/I_D). The decrease in FRET efficiency is a direct indicator of membrane fusion.

Additionally, the FRET efficiency for each ratio of labeled liposomes to unlabeled liposomes, decrease with each freeze-thaw cycle, as evidence from the results in (Fig.8). This happens because there is a greater dilution of the membrane with each cycle made, as further events of liposome fusion occur.

In the case of a nearly two-dimensional system (at the FRET scale), such as a membrane bilayer, where FRET donors and acceptors species are found randomly distributed in well-defined planes, analytical solutions are available to determine FRET efficiency values for different acceptor concentrations. The dilutions from the previous experiments can then be quantified from the recovered FRET efficiencies.

In order to estimate FRET efficiencies for a given concentration of donors and acceptors, the Förster radius (R_0) of that donor-acceptor pair must be calculated first:

$$R_0^6 = 8{,}79 \times 10^{-5} \times n^{-4} \times \phi_{\mathrm{D}} \times \kappa^2 \times J \ (R_0 \text{ in Å}^6) \qquad \textbf{Eq. 2}$$

where n is the refractive index, Q_{D} is the donor quantum yield in the absence of the acceptor, κ is the orientational factor, dictated by the relative orientation of donor emission and acceptor excitation momenta. J is the overlap integral between donor emission and acceptor excitation spectra [48]:

$$J = \int_0^\infty I_{\mathrm{D}}(\lambda)\varepsilon_{\mathrm{A}}(\lambda)\lambda^4 d\lambda \ (\lambda \text{ in nm}) \qquad \textbf{Eq. 3}$$

For the donor the donor/acceptor pair used here (DOPE-NBD/DOPE-Rho), the R_0 was determined to be 50 Å.

In the analytical models mentioned above, it is useful to estimate FRET efficiency through integration of fluorescence lifetime of the donor in the presence of the acceptor ($i_{DA}(t)$) and comparison with donor fluorescence decay in the absence of FRET ($i_D(t)$). Since the membrane thickness (40 Å) is smaller than the R_0 (50 Å), energy transfer can also occur between donors and acceptors in opposing leaflets (out-of-plane). The donor decay law in the presence of acceptor becomes [49]:

$$i_{\mathrm{DA}}(t) = i_{\mathrm{D}}(t) \times \prod_{l(same\ leaflet)}^{l(opposing\ leaflet)} \exp\left\{-\pi R_0^2 \gamma\left[\frac{2}{3}, \left(\frac{R_0}{l}\right)^6 \left(\frac{t}{\tau_{\mathrm{D}}}\right)\right]\left(\frac{t}{\tau_{\mathrm{D}}}\right)^{\frac{1}{3}}\right\} \cdot \exp\left\{-\pi l^2\, \sigma_{\mathrm{A}}\left(1 - exp\left[-\left(\frac{R_0}{l}\right)^6 \left(\frac{t}{\tau_{\mathrm{D}}}\right)\right]\right)\right\} \quad \textbf{Eq. 4}$$

where τ_D is the fluorescence lifetime of the donor in the absence of FRET, γ in the incomplete gamma function, σ_A is the acceptor density in each bilayer leaflet, and l is the distance between the plane of donor and each plane of acceptors in the membrane (same or opposing leaflet).

Using the formalisms described above, the corresponding dilution was estimated for each determined FRET efficiency after freeze-thaw cycles of labeled and unlabeled liposomes (Fig.9). The membrane dilution represents the dilution observed after the fusion of the different liposomes and is an indicator of the efficiency of the fusion method. The results show that as the number of freeze-thaw cycles increases, the membrane dilution increases as well. This was observed for all the different ratios.

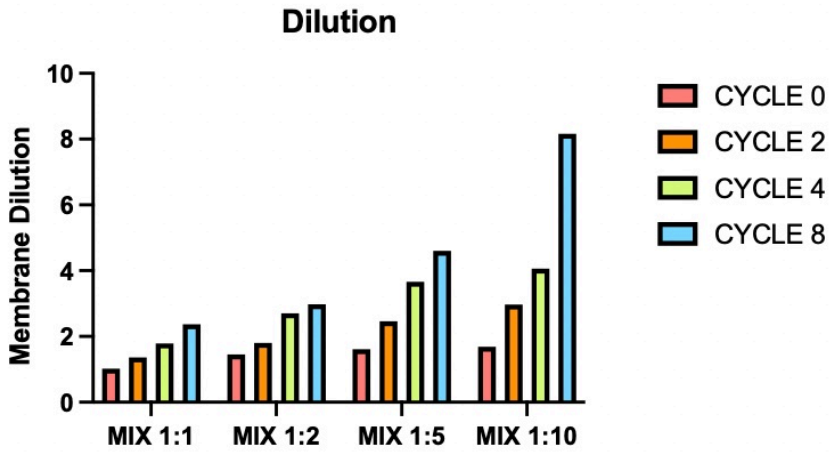

Figure 9 – Membrane dilution.

Theoretically, the maximum dilution that could be obtained from the different ratios 1:1,1:2,1:5 and 1:10 was, respectively, 2, 3, 6 and 11, achieved if all of the liposomes had been efficiently fused.

When looking individually to each ratio (Fig.10) it can be observed that, in the case of the 1:1 ratio the membrane dilution reported for the cycle 8 surpassed the expected theoretical maximum, indicated as a dotted line. This can be explained by measurement errors associated to equipment and inter-experiment variability.

In the case of the 1:2 ratio, the fusion cycle that showed the maximum membrane dilution was the cycle 8. Although 4 cycles did not show as much membrane dilution as 8 cycles of fusion, when choosing between the two, 4 cycles of fusion would be preferable, because it produces almost the same membrane dilution and would subject the EVs to less stress. With the labeled:unlabeled vesicle ratios of 1:5 and 1:10, membrane dilution did not reach the theoretical maximum membrane dilution value, but as reported for the other ratios, dilution also increased with the number of cycles performed.

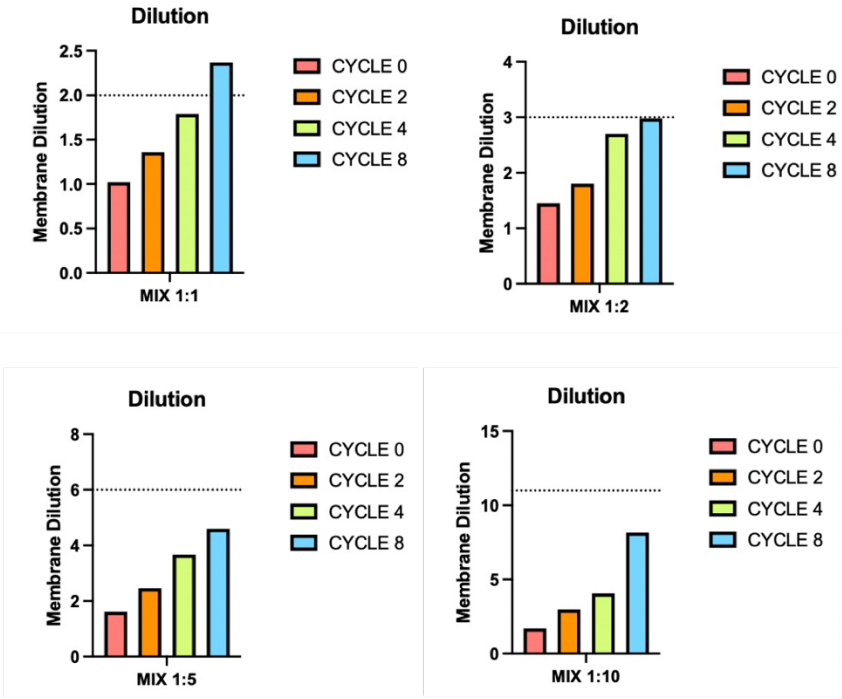

Figure 10 – Membrane dilution compared to the maximum theoretical value (dotted line) achievable upon 100% membrane fusion.

The overall results demonstrate that the fluorescent lipids in the labeled liposomes were diluted by the membrane components present in the unlabeled liposomes. A change in the lipid composition of the unlabeled liposomes was achieved with membrane fusion with labeled liposomes. It can be extrapolated that this method can be replicated with EV-liposome fusion with the purpose of engineering EVs with already functionalized liposomes.

In summary, these results indicate that the fusion of liposomes with labeled liposomes was effective, and that the functionalization of unlabeled liposomes with extrinsic characteristics was accomplished.

3.2. Fusion between EVs and fluorescent labeled liposomes

After the fusion between unlabeled liposomes and fluorescent labeled liposomes, the fusion between EVs and fluorescent labeled liposomes was tested. EVs were fused with fluorescent labeled

liposomes by the freeze-thaw method. The fluorescently labeled liposomes were prepared in the same manner as described previously while EVs were produced and isolated from HEK cells as described in the methods section. Liposomes were diluted to 1 μM (BDP/Rho diluted to 0.01 μM). At this concentration, assuming that liposomes of 100 nm are constituted by 1 x 10^5 lipids, an approximated 6 x 10^9 liposomes per mL were estimated using Avogadro's number. EVs were diluted to 10 x 10^9 particles per mL.

EVs were mixed with the labeled liposomes at a volumetric ratio of 1:1 and the FRET efficiency was calculated prior to freeze-thaw (cycle 0) and for cycles 2 and 4 (Fig. 11).

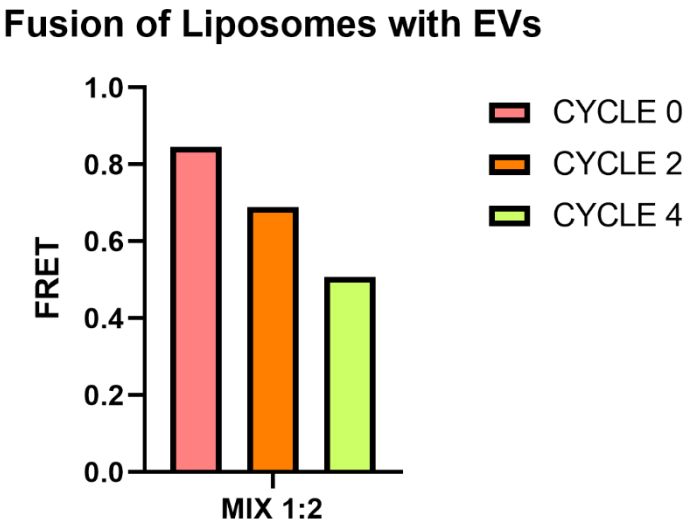

Figure 11 - FRET efficiency of the liposome and EVs mixture was defined as E= 1 - (I_{DA}/I_D). The FRET calculation is a direct indicator of membrane fusion.

The results show that the FRET efficiency for the approximated 1:2 particle ratio of labeled liposomes to EVs, decreases with each freeze-thaw cycle, as evidenced from the results in (Fig.11). This happens because there is a greater dilution of the membrane with each cycle, indicating that the fusion of EVs-liposomes was effective.

The FRET efficiency for the approximated 1:2 particle ratio of labeled liposomes to EVs was very similar to the FRET efficiency observed for the 1:2 ratio of labeled liposomes to unlabeled liposomes, allowing for the assumption that the optimization of the fusion conditions between labeled liposomes and unlabeled liposomes can be extrapolated for the EV-Liposome fusion, and the ideal conditions would be the same.

The corresponding dilution was estimated for each determined FRET efficiency after freeze-thaw cycles of labeled liposomes with EVs. (Fig.12).

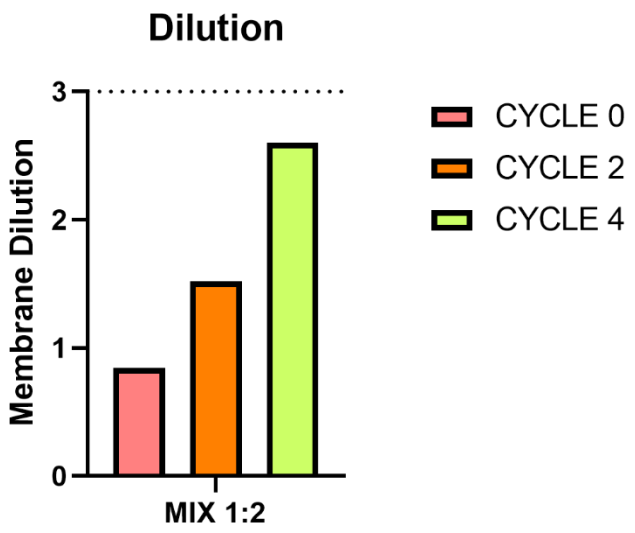

Figure 12 - Membrane dilution compared to the maximum theoretical value (dotted line) achievable upon 100% membrane fusion.

The results show that, as it was observed for the experiments with labeled and unlabeled liposomes, as the number of freeze-thaw cycles increases, the membrane dilution increases as well.

As mentioned previously, the maximum dilution that could be obtained from the ratio 1:2 is 3, assuming that all of the liposomes had been efficiently fused with the EVs. In this particular case, the fusion cycle that showed the maximum membrane dilution was the cycle 4.

The results for the dilution of the 1:2 ratio are once again very similar to the results from the dilution observed with the labeled and unlabeled liposomes, allowing for the assumption that, just like the fusion of liposomes with labeled liposomes, the fusion of labeled liposomes and EVs was effective, and the functionalization of EVs with extrinsic characteristics was accomplished.

3.3. Functionalization of Liposomes

Initially, an azide containing the fluorophore BDP-azide was employed for optimization of the functionalization process. In addition, the functionalization of liposomes was performed with PEG-azide. The liposomes were prepared with POPC and DBCO-PE. As explained in the introduction, by introducing a lipid with a DBCO-PE group in the liposomes composition, the group could be covalently linked to an azide containing molecule. This technique allows for the functionalization of liposomes with different molecules.

The group DBCO-PE absorbs light with a maximum at around 290 nm, and on the other hand, the product of the DBCO-PE-azide reaction does not absorb light, which allows for the reaction with azide to be followed spectroscopically. Alternatively, the fluorescence of liposomes labeled with BDP-azide can also be used to characterize functionalization efficiency.

Different percentages of DBCO-PE lipids were tested, and its modification efficiency was monitored. As it was described previously, the click chemistry reaction in liposomes was executed with different ligand concentration and the reaction was monitored at different reaction times, in order to identify optimum conditions.

The first functionalization experiment was performed by adding the fluorophore BDP-azide to the liposomes containing 25 µM DBCO-PE. The experiment was performed with two different ratios (1:1 and 1:4) of DBCO-PE to BDP-azide (Fig.13, Fig. 14). UV-visible absorption spectroscopy measurements were taken right after the addition of the BDP-azide and then at 3 h, 6 h, and 24 h after the beginning of the reaction. The samples were kept in constant stirring for the whole reaction process.

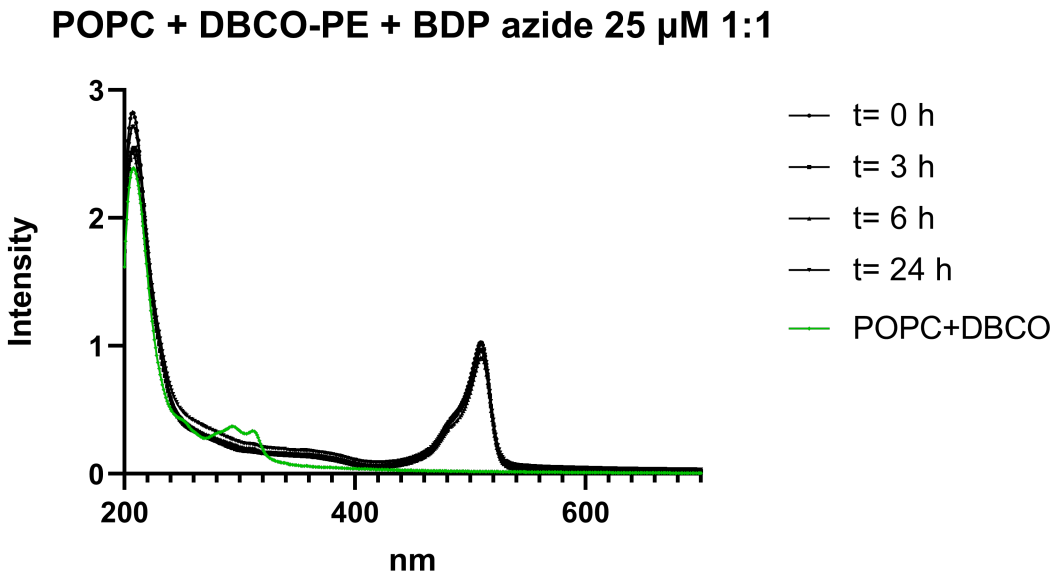

Figure 13 – Absorbance spectra of click chemistry reaction with a 25µM DBCO-PE concentration, a 1:1 proportion of DBCO-PE to BDP-azide and different measurement times.

As it can be observed in Fig.13, the absorbance band of DCBO with a maximum around 290 nm is easily identified from the sample prior incubation with the azide fluorophore. The absorbance spectra from the samples taken at the different reaction times (t= 0, 3, 6, and 24 hours) are very similar, with near complete elimination of the DBCO-PE band. The band associated to the emission maximum of the BDP-azide at 512 nm can also be observed. The results clearly show that when the BDP-azide is added to the solution, the band associated with DBCO-PE disappear immediately.

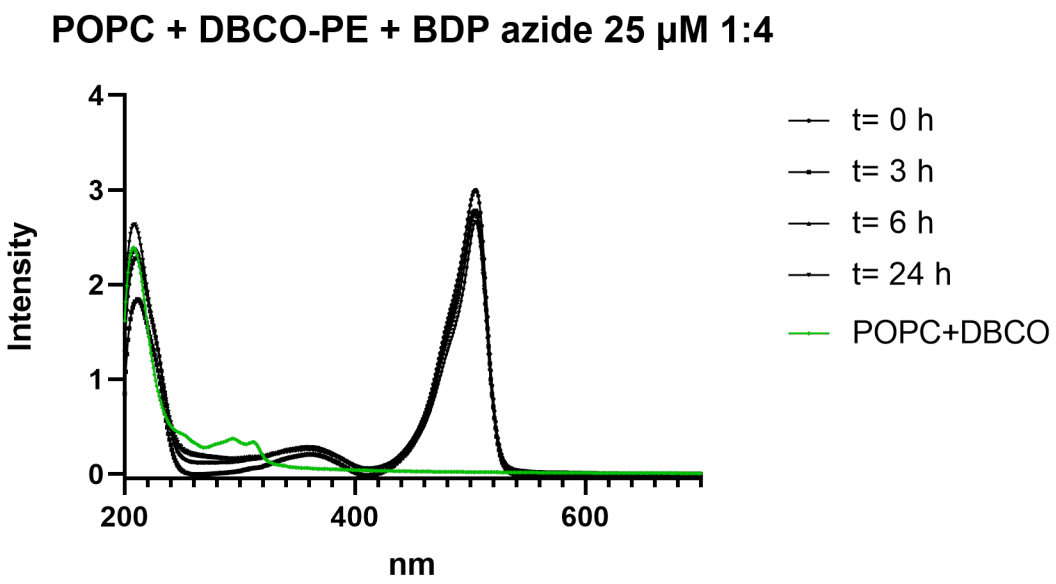

Figure 14 - Absorbance spectra of click chemistry reaction with a 25 µM DBCO-PE concentration, a 1:4 proportion of DBCO-PE to BDP-azide and different measurement times.

The same situation was observed in the samples with the 1:4 ratio of DBCO-PE to BDP-azide. The absorbance spectra from the samples taken at the different reaction times (t= 0, 3, 6, and 24 hours) did not vary significantly, and the spectrum of POPC and DBCO-PE (line in green, prior to incubation with azide fluorophore) shows the band that indicates the presence of the DBCO-PE, which disappears immediately after the addition of BDP-azide.

The results above suggest that the click chemistry reaction between the DBCO-PE groups and the fluorophore BDP-azide was extremely efficient resulting in all of the DBCO-PE groups ligated to BDP-azide molecules, immediately after the onset of reaction. Such a fast reaction, implies that BDP-azide readily translocate to the inner leaflet of the vesicle and react with DBCO-PE groups located there ,which are expected to correspond to roughly 50% of total available. This is not unexpected, since BDP-azide is a fairly hydrophobic molecule.

After the click chemistry reaction, two of the samples (POPC+DBCO-PE+BDP-azide 6 h 1:1 and 1:4) were run through SEC, to exclude any nonbinding BDP-azide that is present in the samples. The results from the purification are demonstrated in the following fluorescence emission spectra (Fig.15, Fig 16).

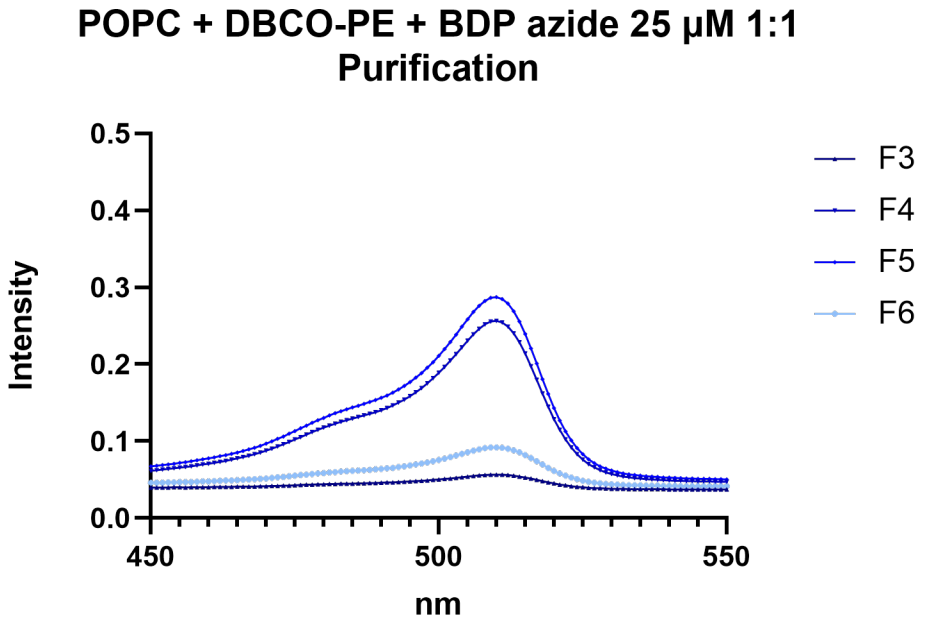

Figure 15 – Absorbance spectra depicting purification through SEC of the sample POPC+DBCO-PE+BDP-azide 25 µM 1:1.F3, F4, F5 and F6 correspond to the various fractions that were eluted from SEC.

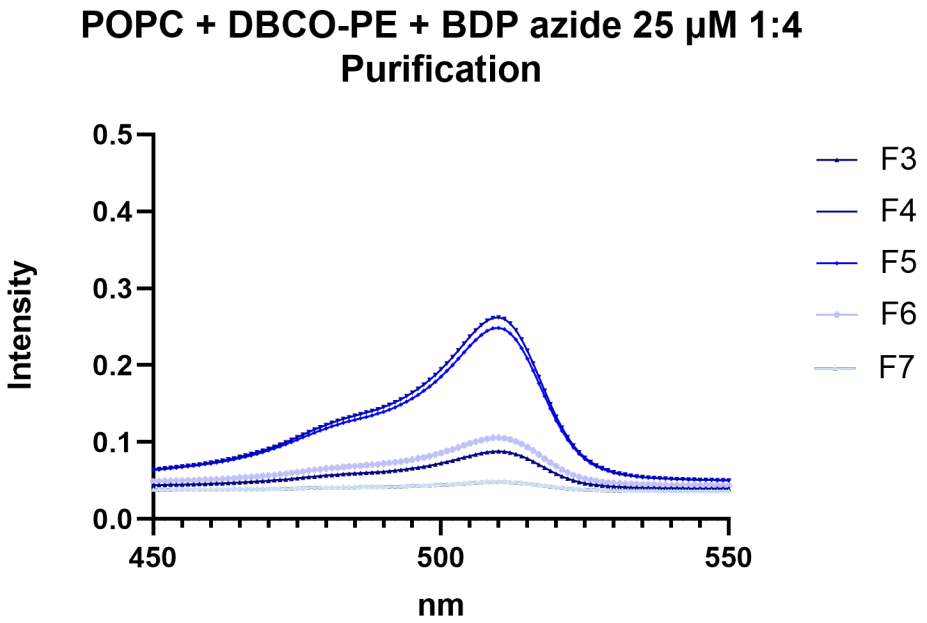

Figure 16 – Absorbance spectra depicting purification through SEC of the sample POPC+DBCO-PE+BDP-azide 25 µM 1:4. F3, F4, F5, F6, F7 correspond to the various fractions that were eluted from SEC.

In both cases, the fractions that show the greater amount of BDP-azide presence are the fractions 4 and 5, identified by the higher fluorescence intensity recorded for these two fractions at 512 nm, the emission maximum of the BDP-azide.

A significant amount of unconjugated BDP-azide was retained in the column as shown in Fig.17, demonstrating that the column allowed effective remotion of BDP-azide added in excess and that the remaining signals observed were from BDP-azide groups ligated to the DBCO-PE groups in the liposomes.

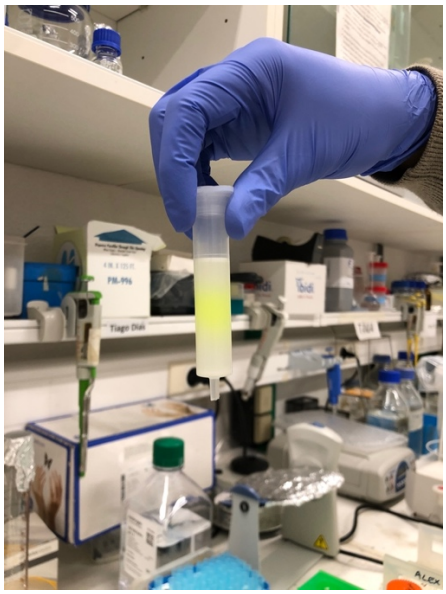

Figure 17 - SEC column with the unconjugated BDP-azide retained shown in yellow.

After the purification, the mixtures were also analysed by NTA for the evaluation of hybrid vesicle heterogeneity. The results are described in the following graphics. (Fig.18)

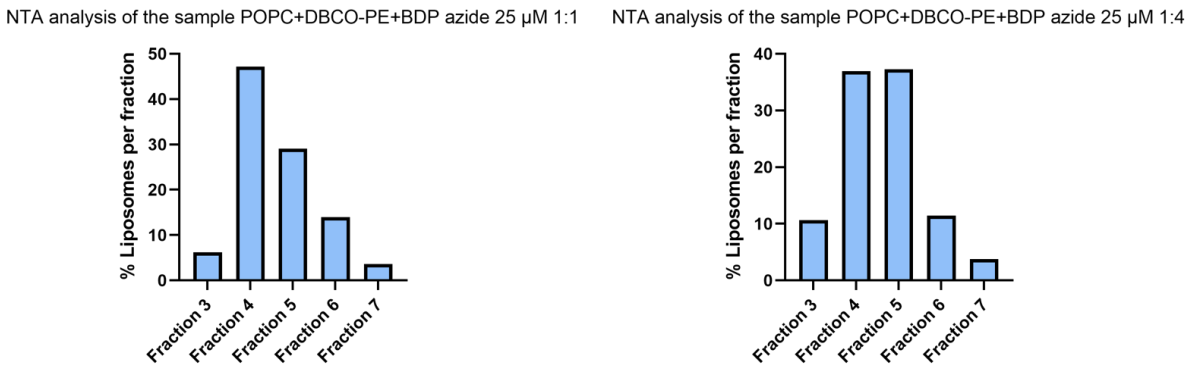

Figure 18 - NTA analysis of the samples POPC+DBCO-PE+BDP-azide 25 µM 1:1 and 1:4.

With this information it is possible to corroborate what was observed by fluorescence. The fractions with the higher percentage of liposomes were indeed the fractions number 4 and 5, in both

reactions (1:1 and 1:4). The total percentage of liposomes that comprises these two fractions are 76.2% and 74.2% for the 1:1 and 1:4 ratios, respectively.

A second click chemistry experiment was performed using BDP-azide as the azide containing fluorophore, but in this case, and in order to identify optimum reaction conditions, the concentration of DBCO-PE used was lower (10 μM).

UV-visible absorption spectroscopy measurements were taken right after the addition of the BDP-azide and 1 hour after the beginning of the reaction. The samples were also kept in constant stirring for the whole reaction process.

The following Fig.19 shows the spectrums from the samples taken prior the onset of reaction and at the two different reaction times (t= 0 and 1 hour). Once more, DBCO-PE absorbance disappears immediately after the onset of reaction and the two absorbance spectra taken after initiation of reaction are essentially the same, indicating that the conditions of the reaction did not vary from the beginning to the end of the click chemistry reaction. The band associated to the emission maximum of the BDP-azide at 512 nm, and the band associated to the DBCO-PE on the spectrum of POPC and DBCO-PE (line in black) can be easily identified. As seen before, reaction between BDP-azide and DBCO-PE was extremely efficient resulting in all of the DBCO-PE groups ligated to BDP-azide molecules, immediately after the onset of reaction.

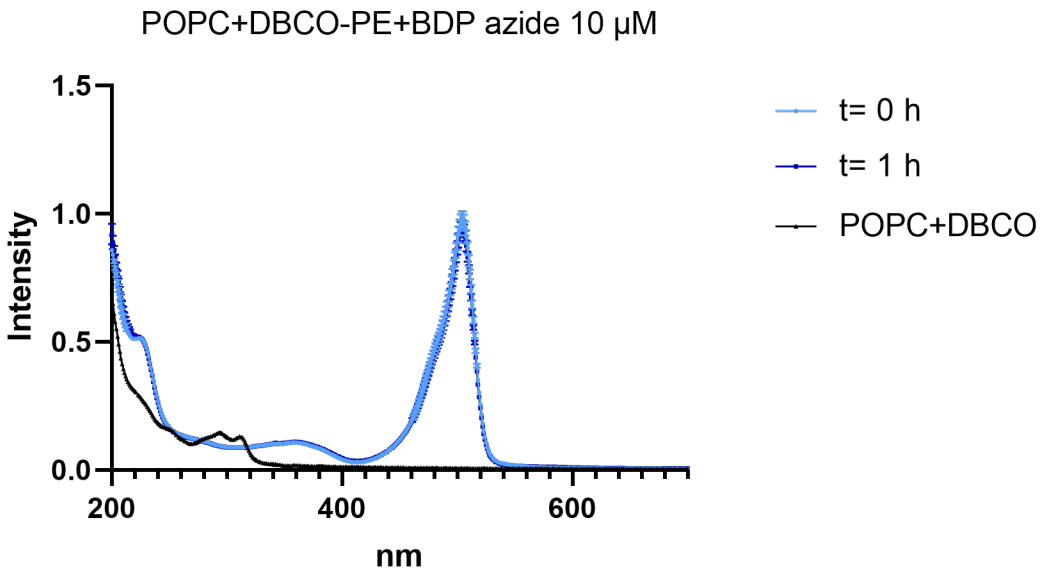

Figure 19 – Absorbance spectra of click chemistry reaction with a 10 μM DBCO-PE concentration and different measurement times.

After the click chemistry reaction, an alternative purification method was tested to purify the liposome samples. Purification with a centrifugal filter unit was performed to exclude any free BDP-azide from the samples. The results from the purification are demonstrated in the following graphic (Fig.20).

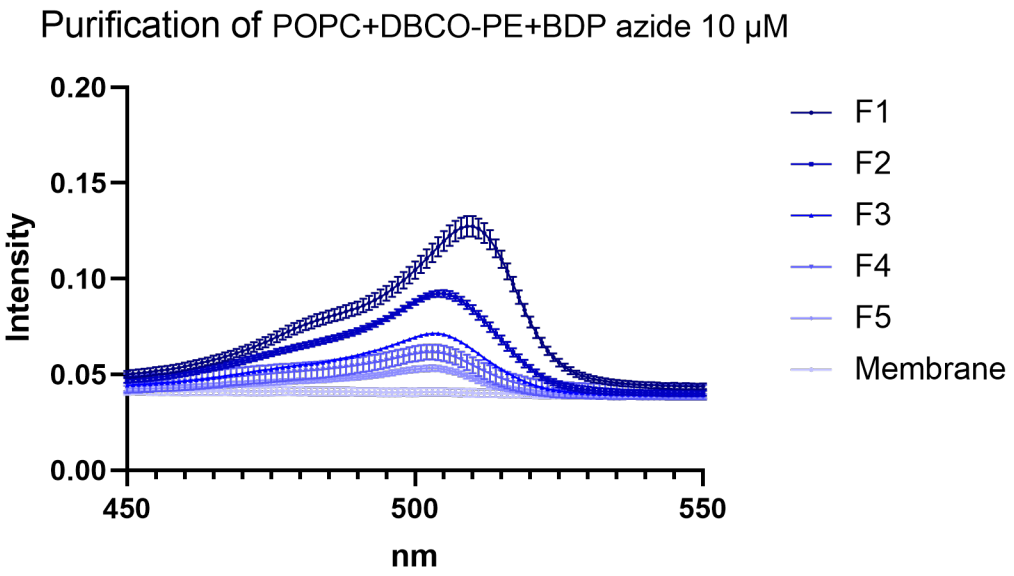

Figure 20 – Absorbance spectra of purification with the centrifugal filter unit of the sample POPC+DBCO-PE+BDP-azide 10 µM. F1, F2, F3, F4 and F5 correspond to the various fractions that were collected. The membrane fraction corresponds to the sample recovered after the purification process.

After the purification with the centrifugal filter unit, fluorescence measurements were taken and the results from Fig.20 show that the more centrifugal runs are executed the lower is the intensity of the BDP-azide signal in the samples, and surprisingly, after multiple runs, almost all BDP-azide fluorescence was lost.

These mixtures were also analysed by NTA for hybrid vesicle heterogeneity, and the results are described in the following graphic (Fig.21).

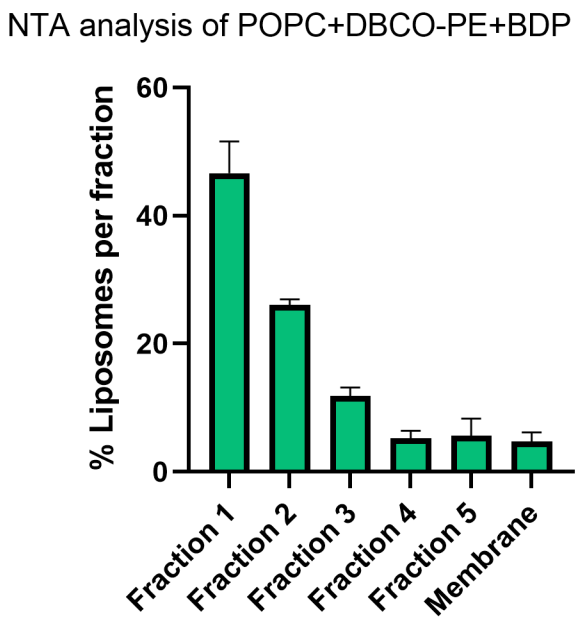

Figure 21 - NTA analysis of the samples POPC+DBCO-PE+BDP-azide 10 µM.

The percentage of liposomes decreased significantly after the first run of centrifugal purification. After these washes the samples should have lost BDP-azide and not liposomes. If the experiment occurred as expected, the fractions recovered from the filter units would be the fractions that should have the liposomes without the free BDP-azide that had been washed out. Since the only fractions that show a significant percentage of liposomes are the first two fractions, it can be concluded that centrifugal runs result in elimination of liposomes, which is undesirable. Since this method does not allow for the recovery of the liposomes, the SEC method was chosen as the ideal method for the purification of the liposome samples.

3.4. Live imaging of Click Chemistry

In order to have a more visual representation of what was happening while the click chemistry reaction was occurring, Giant unilamellar vesicles (GUV´s) with a lipid composition of POPC, DBCO-PE and DOPE-Rho, 97.33:1.67:1 mol:mol:mol were used. DOPE-Rho was used to visualize vesicles before the onset of reaction with BDP-azide. BDP-azide was added to the GUV's while measuring their fluorescence between 490 - 530 nm with confocal laser scanning fluorescence microscopy.

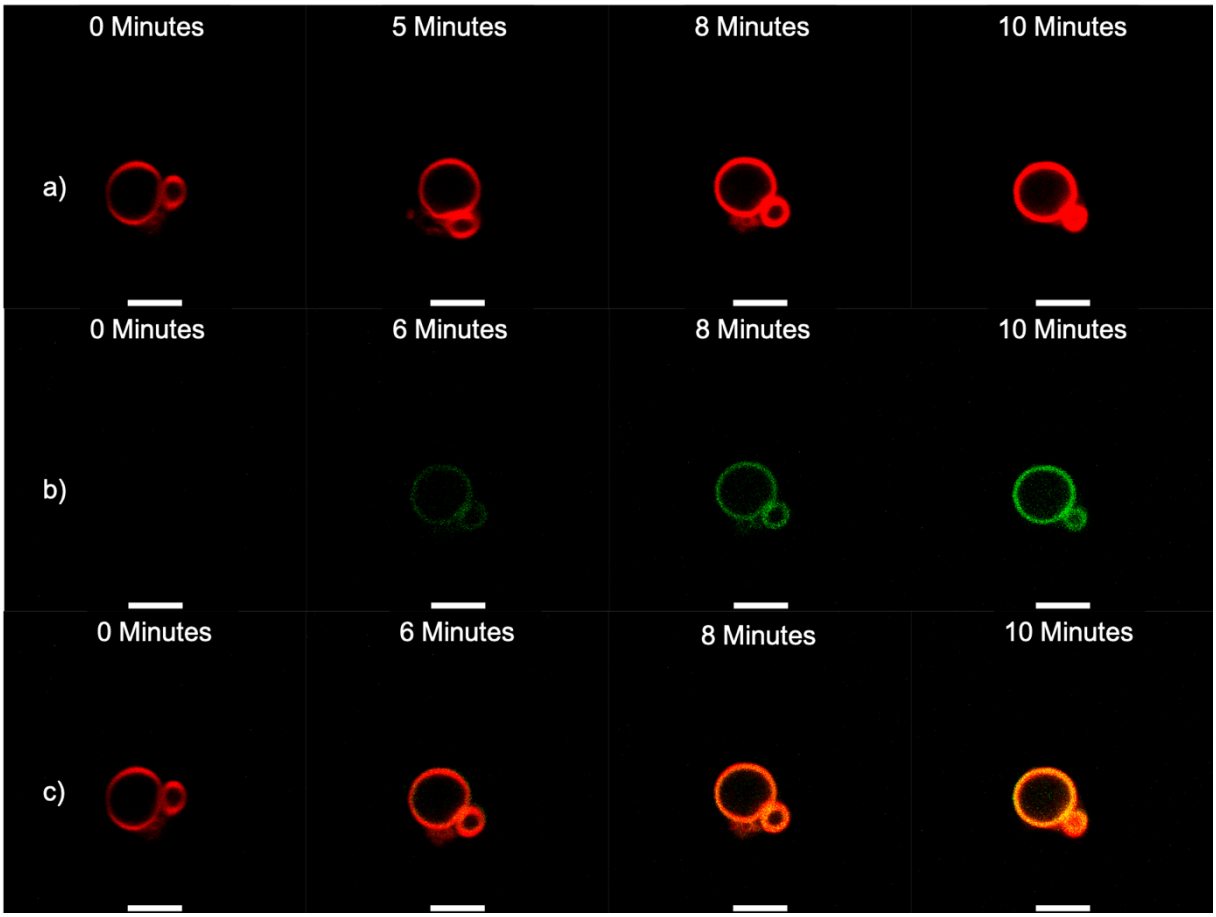

Figure 22 – Three different channels, a), b) and c). The channel a) is the red channel, representative of the Rho, channel b) is the green channel, representative of the BDP-azide, and the channel c) corresponds to the merge of the first two channels. Each channel has four frames, taken at different times, that show a live click chemistry 10 minutes reaction between the BDP-azide and the DBCO-PE groups on the vesicles. DOPE-Rho fluorescence is shown in red and BDP-azide fluorescence is show in green. Scale bar: 5μM.

It can be observed that in a matter of minutes, the liposome exhibited considerable BDP-azide fluorescence, indicating a successful click chemistry reaction. In Fig. 22, the evolution of the click chemistry reaction is represented at 4 different times per each channel.

3.5. Functionalization of Liposomes with PEG-azide

After the functionalization of liposomes with BDP-azide, the functionalization of liposomes was performed with PEG-azide. The liposomes were, once again, prepared with POPC and DBCO-PE. As mentioned previously, DBCO-PE absorbs light with a maximum at around 290 nm. In addition, PEG-azide has no UV-absorption, therefore this molecule does not interfere with monitorization of the reaction.

The first reaction of click chemistry with PEG-azide in liposomes was executed with different DBCO-PE concentration (0.25, 0.5, 1 and 2 μM) and the reaction was monitored at different reaction

times (0, 1 and 3 hours), in order to identify optimum reaction conditions (Fig. 23). The samples were kept in constant stirring for the whole reaction process.

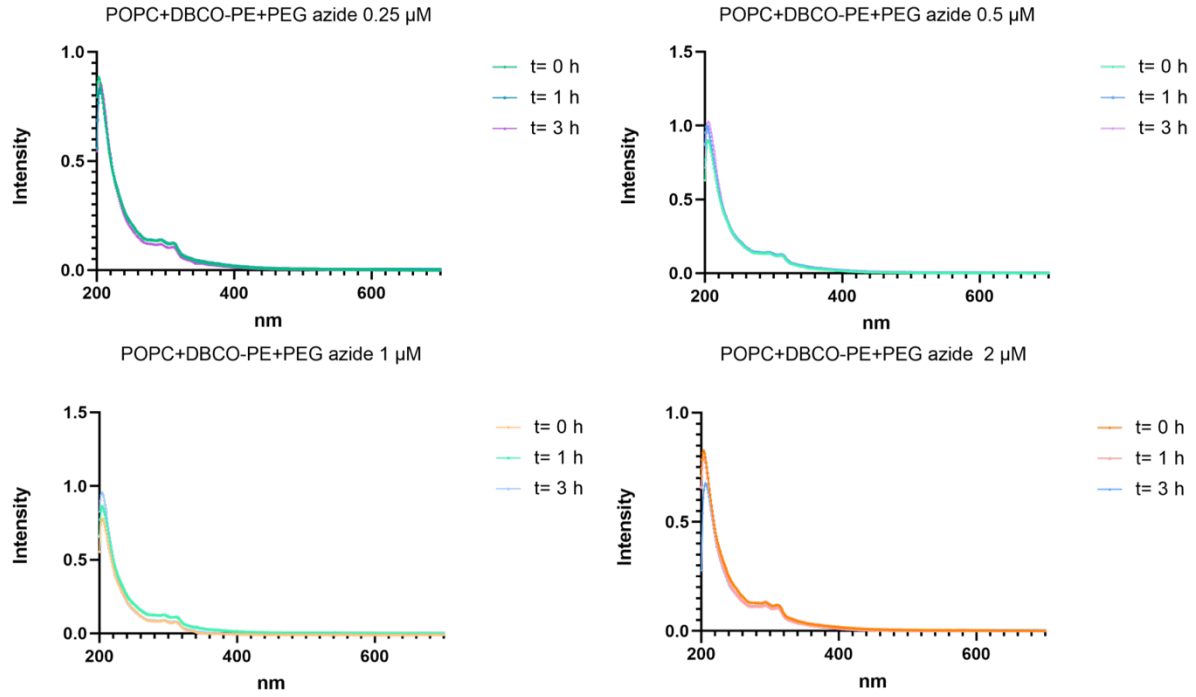

Figure 23 – Absorbance spectra of click chemistry reaction with POPC+DBCO-PE at 0.25 µM, 0.5 µM, 1 µM and 2 µM reacting with PEG-azide.

In all of the different conditions discriminated in the graphics above (0.25, 0.5, 1 and 2 µM), the spectra hardly changed from the first measurement to the last, 3 hours later.

The representative band of DBCO-PE was observed in all of the conditions at around 290 nm, and because the product of the DBCO-PE-azide reaction does not absorb light, it can be concluded that the functionalization did not occur.

Airoldi *et al.*[50] suggested that the best results for this reaction would be obtained after 48 h of incubation, and with that in mind, the functionalization of the liposomes with PEG-azide (n=3) in two different concentrations (10µM and 25µM) was performed, and measurements were taken at times 0h, 3 h, 6 h, 24 h and 48 h after the beginning of the click chemistry reaction. The results obtained are shown in the Fig.24 and Fig.25.

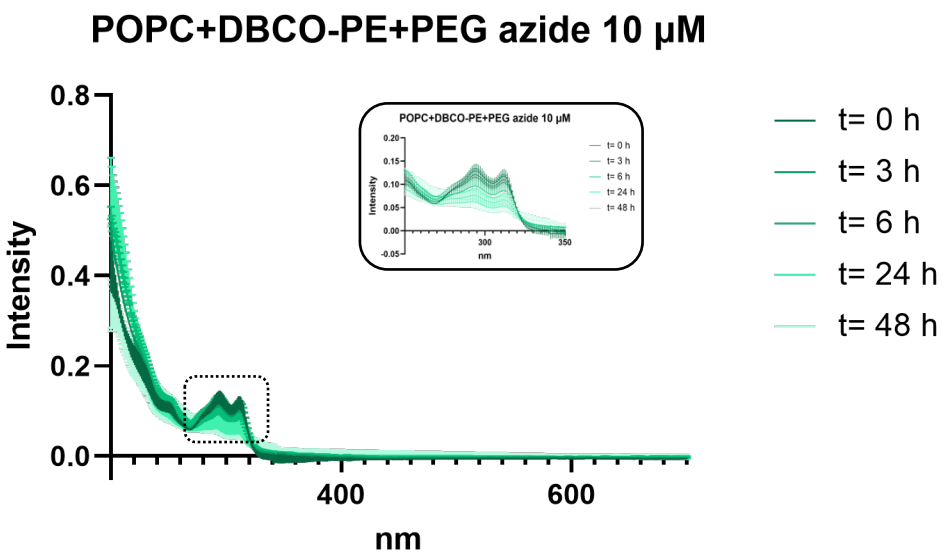

Figure 24- Absorbance spectra of click chemistry reaction with a 10µM DBCO-PE concentration, PEG azide and different measurement times.

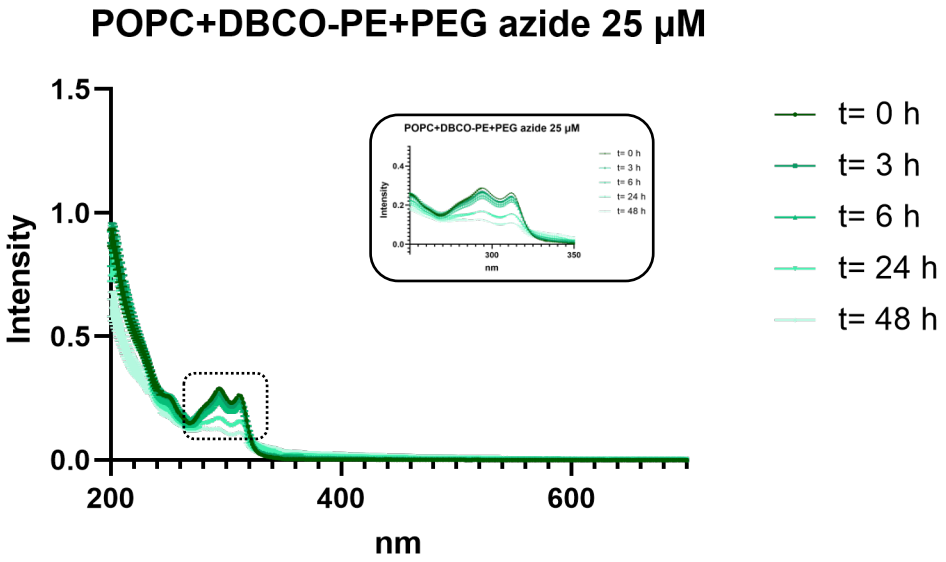

Figure 25 – Absorbance spectra of click chemistry reaction with a 25µM DBCO-PE concentration, PEG azide and different measurement times.

Table 1 – Percentages of functionalization of the liposomes with PEG-azide in two different concentrations (10μM and 25μM) after 3h, 6h, 24h and 48h.

	3h	6h	24h	48h
10μM	7.69 %	7.69 %	38.46 %	53.85 %
25μM	6.90 %	13.79 %	41.38 %	55.17 %

What can be concluded from both of this graphics is that, unlike the functionalization with the BDP-azide, the functionalization with PEG-azide was dramatically slower. Nevertheless, functionalization can be observed as the band from the DBCO-PE decreases significantly overtime. A more significant decrease in the DBCO-PE absorbance occurs only after 24 hours of reaction, meaning that the functionalization only started to occur many hours after the beginning of the reaction.

As shown in table 1, after 48 h, around 50% of functionalization is achieved. This is the maximum functionalization expected, since a little less than half of the DBCO-PE groups are facing inwards the liposome membrane and therefore are not available to react with the PEG-azide.

The functionalization efficiency with the PEG-azide is very different from the functionalization efficiency with BDP-azide because the fluorophore BDP-azide is an hydrophobic compound that has the ability to translocate to the inside of the vesicle and react with all the DBCO-PE groups.

3.6. The study of the activity of Neprilysin (NEP) with ECE1-substrate

Since freeze-thaw cycles can potentially lead to enzyme denaturation, the study of the activity of the enzyme Neprilysin with ECE-1-substrate after being subjected to freeze-thaw cycles was performed.

The ECE-1 substrate is an internally quenched fluorogenic substrate that can be cleaved by NEP and IDE [51,52]. This peptide contains a fluorophore (MCA; FRET donor) that has an emission spectrum that overlaps with the absorbance spectrum of a quencher (DNP; FRET acceptor), also contained in the peptide, resulting in a transference of energy between the fluorophore and the acceptor that quenches the donor fluorescence. When the peptide is cleaved at any position, the separation of the fluorophore and FRET acceptor eliminates FRET, and an increase in the signal is observed (Fig. 26)[48]. By monitoring the fluorescence intensity of this peptide, it is possible to evaluate the activity of a protease. The maximum fluorescence intensity is reached when there is no more substrate for the enzyme.

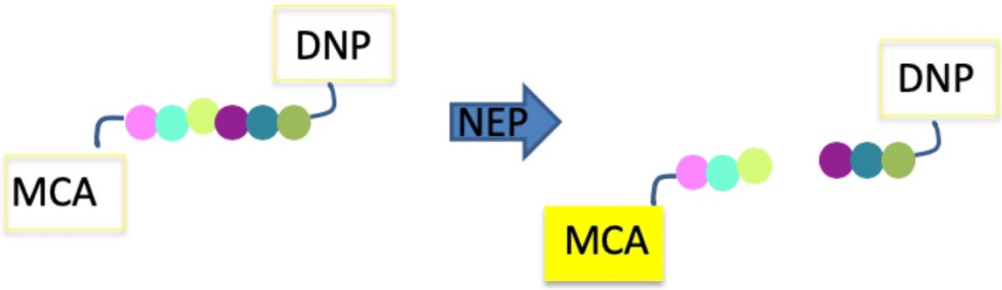

Figure 26 - *Hydrolyzation of ECE-1 substrate by NEP (Adapted from Lakowicz et.al)* [48].

In this experiment, purified porcine NEP's activity was tested using ECE-1 substrate. This enzyme does not cut peptides with high specificity and always in the same region. This allowed for the study and optimization of the conditions at which the enzyme has more activity using a generic protease substrate such as the ECE-1 peptide. With this method, the ability of NEP to successfully cleave ECE-1 was studied.

If, as mentioned previously, for the fusion of different liposomes, the 1:2 ratio and the cycle 4 were chosen as the optimum conditions for a fusion experiment, it would be crucial to know that this enzyme would still be active in these conditions.

In this experiment, four solutions of NEP with PBS buffer were subjected to freeze-thaw cycles (0, 2, 4 and 8 cycles respectively). After the cycles, the ECE1-substrate solution was added to the 4 solutions and measurements were run with 3 replicates for each condition.

Four independent experiments (n=4) of activity studies with ECE1-substrate were performed (Fig. 27).

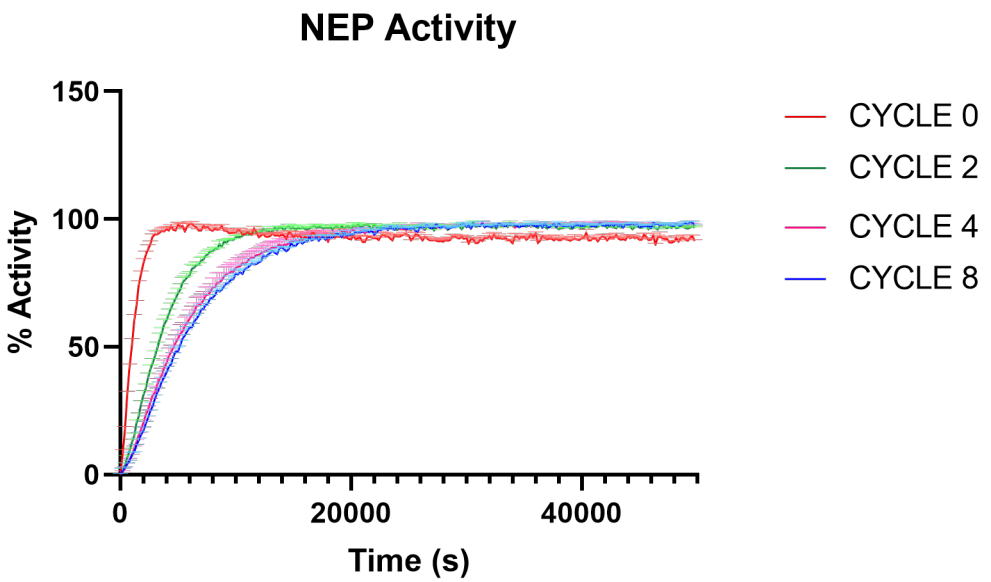

Figure 27 – Study of the activity of the enzyme Neprilysin with ECE-1-substrate after being subjected to the freeze-thaw cycles.

The results from the Fig.27 indicate that, as predicted, MCA fluorescence intensity increases with time, confirming that NEP has indeed activity against ECE-1 substrate. The results also show that as the number of cycles increases, the enzyme neprilysin loses some of its activity, therefore diminishing the final MCA's concentration in solution which results in a lower value of MCA fluorescence intensity. This result is to be expected as the freeze-thaw method implies great variations in temperature that could affect the enzyme's activity due to denaturation. Nonetheless, the NEP enzyme retained significant activity after 8 cycles of freeze-thaw, which is very positive, as a relatively large number of freeze-thaw cycles can be used during fusion and functionalization experiment, without loss of most NEP activity.

Following the study of the activity of the enzyme Neprilysin with ECE-1-substrate after being subjected to the freeze-thaw cycles, the same experiment was performed but with EVs engineered to overexpress Neprilysin. The purpose of this second experiment was also to understand the potential negative impact of freeze-thaw on enzyme activity and to compare this impact when the enzyme is free or incorporated in the EVs.

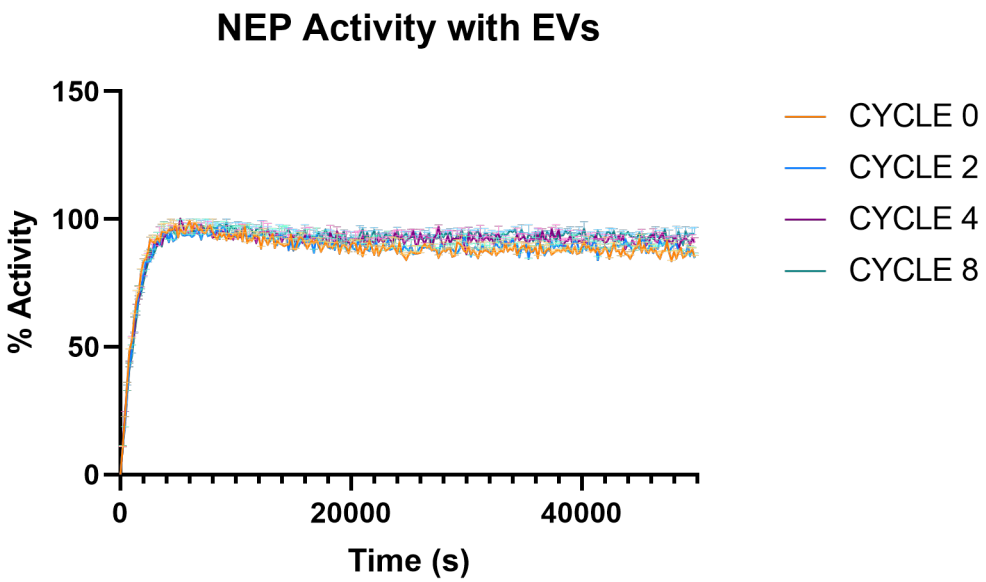

Figure 28 - Study of the activity of the enzyme Neprilysin in EVs with ECE-1-substrate after being subjected to the freeze-thaw cycles.

The results from the NEP activity studies made with EVs (n=2) are shown in Fig.28 and they present a much more consistent activity throughout the cycles than the purified free NEP enzyme, suggesting no impact whatsoever of the freeze-thaw cycles on enzyme activity. This could be due to NEP being more protected from external conditions by being incorporated in the membrane of EVs, which reduces the probability of denaturation during freezing.

IV. Conclusion

Regarding the fusion between unlabeled liposomes and fluorescent labeled liposomes it can be concluded that the freeze-thaw technique was effective and that the functionalization of unlabeled liposomes with extrinsic characteristics was accomplished. This was the first step into the functionalization of liposomes and exosomes.

The fusion between EVs and fluorescent labeled liposomes was also tested and the results showed that this fusion was effective, confirming the possibility of using this methodology to engineer hybrid EVs with already functionalized liposomes.

The functionalization of liposomes by click chemistry reaction between the DBCO-PE groups and the fluorophore BDP-azide was extremely efficient resulting in all of the DBCO-PE groups ligated to BDP-azide molecules. After witnessing the live click chemistry reaction, it could be concluded that part of the reason why the reaction was so effective was because the BDP-azide is hydrophobic, which might lead to the ability to translocate the phospholipid bilayer membrane of the GUV's, associate to the membrane and ligate to the DBCO-PE groups that are directed inwards of the vesicle, that otherwise would be unreachable. The functionalization of liposomes with PEG-azide showed considerably lower efficiency than functionalization with BDP-azide, and a much longer reaction time was necessary to achieve significant functionalization. The introduction and functionalization of the DBCO-PE group indicates that any peptide conjugated with an azide group can be bound to liposomes and then fused to EVs, opening a world of possibilities regarding EVs functionalization.

The last step of this thesis consisted in activity studies of the enzyme NEP, which presented significant activity when subjected to multiple freeze-thaw cycles. NEP activity from the enzyme within EVs was shown to be much more resistant to freeze-thaw cycles than the activity of soluble purified enzyme. The fact that NEP did not lose activity when subjected to the different freeze-thaw cycles while incorporated in the EVs membrane, suggest that if EVs bearing NEP in their membrane were functionalized by fusion with liposomes, the enzyme would still be active after the cycles and could potentially exert its capacity as a β-amyloid peptide-degrading enzyme preventing pathogenic changes in the brain. In this way, production of hybrid EV/liposome particles through the freeze-thaw technique is ideal to achieve further functionalization of NEP-loaded EVs, which could be employed in therapeutic applications in the context of Alzheimer's disease. The same methodology is likely to be successful in achieving EV functionalization for other applications. The simplicity of the procedure is a considerable advantage over alternative methods to achieve functionalization. Through control of liposome composition, extraordinary control of final EV functionalization pattern is possible. However, it is not entirely clear yet if the hybrid vesicles produced as described here retain all of the advantageous properties of EVs and further research will be necessary to clarify this issue.

V. References

1. Ohno SI, Drummen GPC, Kuroda M. Focus on extracellular vesicles: Development of extracellular vesicle-based therapeutic systems. *Int J Mol Sci*. 2016;17(2). doi:10.3390/ijms17020172

2. Borges FT, Reis LA, Schor N. Extracellular vesicles: Structure, function, and potential clinical uses in renal diseases. *Brazilian J Med Biol Res*. 2013;46(10):824-830. doi:10.1590/1414-431X20132964

3. Gutierrez-Millan C, Calvo Díaz C, Lanao JM, Colino CI. Advances in Exosomes-Based Drug Delivery Systems. *Macromol Biosci*. Published online 2020. doi:10.1002/mabi.202000269

4. Doyle LM, Wang MZ. Overview of Extracellular Vesicles, Their Origin, Composition, Purpose, and Methods for Exosome Isolation and Analysis. *Cells*. Published online 2019. doi:https://dx.doi.org/10.3390/cells8070727

5. Ciardiello C, Cavallini L, Spinelli C, et al. Focus on extracellular vesicles: New frontiers of cell-to-cell communication in cancer. *Int J Mol Sci*. 2016;17(2):1-17. doi:10.3390/ijms17020175

6. Van Niel G, D'Angelo G, Raposo G. Shedding light on the cell biology of extracellular vesicles. *Nat Rev Mol Cell Biol*. 2018;19(4):213-228. doi:10.1038/nrm.2017.125

7. Gangadaran P, Ahn BC. Extracellular vesicle-and extracellular vesicle mimetics-based drug delivery systems: New perspectives, challenges, and clinical developments. *Pharmaceutics*. 2020;12(5). doi:10.3390/pharmaceutics12050442

8. Zaborowski MP, Balaj L, Breakefield XO, Lai CP. Extracellular Vesicles: Composition, Biological Relevance, and Methods of Study. *Bioscience*. 2015;65(8). doi:10.1093/biosci/biv084

9. Xu R, Greening DW, Zhu HJ, Takahashi N, Simpson RJ. Extracellular vesicle isolation and characterization: Toward clinical application. *J Clin Invest*. 2016;126(4):1152-1162. doi:10.1172/JCI81129

10. Kalra H, Drummen GPC, Mathivanan S. Focus on extracellular vesicles: Introducing the next small big thing. *Int J Mol Sci*. 2016;17(2). doi:10.3390/ijms17020170

11. Srivastava A, Amreddy N, Pareek V, et al. Progress in extracellular vesicle biology and their application in cancer medicine. *Wiley Interdiscip Rev Nanomedicine Nanobiotechnology*. 2020;12(4). doi:10.1002/wnan.1621

12. Ha D, Yang N, Nadithe V. Exosomes as therapeutic drug carriers and delivery vehicles across biological membranes: current perspectives and future challenges. *Acta Pharm Sin B*. 2016;6(4). doi:10.1016/j.apsb.2016.02.001

13. Patil SM, Sawant SS, Kunda NK. Exosomes as drug delivery systems: A brief overview and progress update. *Eur J Pharm Biopharm*. 2020;154. doi:10.1016/j.ejpb.2020.07.026

14. Khan AA, Allemailem KS, Almatroodi SA, Almatroudi A, Rahmani AH. Recent strategies towards the surface modification of liposomes: an innovative approach for different clinical applications. *3 Biotech*. 2020;10(4). doi:10.1007/s13205-020-2144-3

15. Li M, Du C, Guo N, et al. Composition design and medical application of liposomes. *Eur J Med Chem*. 2019;164. doi:10.1016/j.ejmech.2019.01.007

16. Ahmed KS, Hussein SA, Ali AH, Korma SA, Lipeng Q, Jinghua C. Liposome: composition, characterisation, preparation, and recent innovation in clinical applications. *J Drug Target*. 2019;27(7). doi:10.1080/1061186X.2018.1527337

17. Lamichhane N, Udayakumar TS, D'Souza WD, et al. Liposomes: Clinical applications and potential for image-guided drug delivery. *Molecules*. 2018;23(2). doi:10.3390/molecules23020288

18. El-Amouri SS, Zhu H, Yu J, Marr R, Verma IM, Kindy MS. Neprilysin: An enzyme candidate to slow the progression of Alzheimer's disease. *Am J Pathol*. 2008;172(5):1342-1354. doi:10.2353/ajpath.2008.070620

19. Campion D, Dumanchin C, Hannequin D, et al. Early-onset autosomal dominant Alzheimer disease: Prevalence, genetic heterogeneity, and mutation spectrum. *Am J Hum Genet*. 1999;65(3):664-670. doi:10.1086/302553

20. Pluta R, Ułamek-Kozioł M, Januszewski S, Czuczwar SJ. Exosomes as possible spread factor and potential biomarkers in Alzheimer's disease: Current concepts. *Biomark Med*. 2018;12(9). doi:10.2217/bmm-2018-0034

21. brightfocus.org. Accessed January 23, 2021. https://www.brightfocus.org/alzheimers-disease/infographic/amyloid-plaques-and-neurofibrillary-tangles

22. Long JM, Holtzman DM. Alzheimer Disease: An Update on Pathobiology and Treatment Strategies. *Cell*. 2019;179(2). doi:10.1016/j.cell.2019.09.001

23. Mishra S, Blazey TM, Holtzman DM, et al. Longitudinal brain imaging in preclinical Alzheimer disease: Impact of APOE ϵ4 genotype. *Brain*. 2018;141(6):1828-1839. doi:10.1093/brain/awy103

24. Cummings JL, Morstorf T, Zhong K. Alzheimer's disease drug-development pipeline: Few candidates, frequent failures. *Alzheimer's Res Ther*. 2014;6(4):1-7. doi:10.1186/alzrt269

25. Awasthi M, Singh S, Pandey VP, Dwivedi UN. Alzheimer's disease: An overview of amyloid beta dependent pathogenesis and its therapeutic implications along with in silico approaches emphasizing the role of natural products. *J Neurol Sci*. 2016;361:256-271. doi:10.1016/j.jns.2016.01.008

26. Ferrantelli F, Chiozzini C, Leone P, Manfredi F, Federico M. Engineered extracellular vesicles/exosomes as a new tool against neurodegenerative diseases. *Pharmaceutics*.

2020;12(6). doi:10.3390/pharmaceutics12060529

27. Selkoe DJ. Alzheimer disease and aducanumab: adjusting our approach. *Nat Rev Neurol*. 2019;15(7):365-366. doi:10.1038/s41582-019-0205-1

28. Mullard A. Landmark Alzheimer's drug approval confounds research community. *Nature*. 2021;594(7863):309-310. doi:10.1038/d41586-021-01546-2

29. Zheng M, Huang M, Ma X, Chen H, Gao X. Harnessing Exosomes for the Development of Brain Drug Delivery Systems. *Bioconjug Chem*. 2019;30(4). doi:10.1021/acs.bioconjchem.9b00085

30. Yasojima K, McGeer EG, McGeer PL. Relationship between beta amyloid peptide generating molecules and neprilysin in Alzheimer disease and normal brain. *Brain Res*. 2001;919(1). doi:10.1016/S0006-8993(01)03008-6

31. Poirier R, Wolfer DP, Welzl H, et al. Neuronal neprilysin overexpression is associated with attenuation of Aβ-related spatial memory deficit. *Neurobiol Dis*. 2006;24(3). doi:10.1016/j.nbd.2006.08.003

32. Kim H, Kim D, Nam H, Moon S, Kwon YJ, Lee JB. Engineered extracellular vesicles and their mimetics for clinical translation. *Methods*. 2020;177. doi:10.1016/j.ymeth.2019.10.005

33. Familtseva A, Jeremic N, Tyagi SC. Exosomes: cell-created drug delivery systems. *Mol Cell Biochem*. Published online 2019. doi:10.1007/s11010-019-03545-4

34. Donoso-Quezada J, Ayala-Mar S, González-Valdez J. State-of-the-art exosome loading and functionalization techniques for enhanced therapeutics: a review. *Crit Rev Biotechnol*. 2020;40(6). doi:10.1080/07388551.2020.1785385

35. Rayamajhi S, Aryal S. Surface functionalization strategies of extracellular vesicles. *J Mater Chem B*. 2020;8(21). doi:10.1039/d0tb00744g

36. Lamichhane TN, Raiker RS, Jay SM. Exogenous DNA loading into extracellular vesicles via electroporation is size-dependent and enables limited gene delivery. *Mol Pharm*. 2015;12(10):3650-3657. doi:10.1021/acs.molpharmaceut.5b00364

37. Luan X, Sansanaphongpricha K, Myers I, Chen H, Yuan H, Sun D. Engineering exosomes as refined biological nanoplatforms for drug delivery. *Acta Pharmacol Sin*. 2017;38(6). doi:10.1038/aps.2017.12

38. Yamawaki M, Zurbriggen A, Richard A, Vandevelde M. Saponin treatment for in situ hybridization maintains good morphological preservation. *J Histochem Cytochem*. 1993;41(1):105-109. doi:10.1177/41.1.8417105

39. Lee J, Lee H, Goh U, et al. Cellular Engineering with Membrane Fusogenic Liposomes to Produce Functionalized Extracellular Vesicles. *ACS Appl Mater Interfaces*. 2016;8(11).

doi:10.1021/acsami.6b01315

40. Gao J, Dong X, Wang Z. Generation, purification and engineering of extracellular vesicles and their biomedical applications. *Methods*. 2020;177. doi:10.1016/j.ymeth.2019.11.012

41. Piffoux M, Silva AKA, Wilhelm C, Gazeau F, Tareste D. Modification of Extracellular Vesicles by Fusion with Liposomes for the Design of Personalized Biogenic Drug Delivery Systems. *ACS Nano*. 2018;12(7). doi:10.1021/acsnano.8b02053

42. Sato YT, Umezaki K, Sawada S, et al. Engineering hybrid exosomes by membrane fusion with liposomes. *Sci Rep*. 2016;6. doi:10.1038/srep21933

43. Takayama Y, Kusamori K, Nishikawa M. Click chemistry as a tool for cell engineering and drug delivery. *Molecules*. 2019;24(1). doi:10.3390/molecules24010172

44. Smyth T, Petrova K, Payton NM, et al. Surface functionalization of exosomes using click chemistry. *Bioconjug Chem*. 2014;25(10). doi:10.1021/bc500291r

45. Ong SGM, Chitneni M, Lee KS, Ming LC, Yuen KH. Evaluation of extrusion technique for nanosizing liposomes. *Pharmaceutics*. 2016;8(4). doi:10.3390/pharmaceutics8040036

46. Gardiner C, Ferreira YJ, Dragovic RA, Redman CWG, Sargent IL. Extracellular vesicle sizing and enumeration by nanoparticle tracking analysis. *J Extracell Vesicles*. 2013;2(1). doi:10.3402/jev.v2i0.19671

47. de Almeida Fuzeta M, Bernardes N, Oliveira FD, et al. Scalable Production of Human Mesenchymal Stromal Cell-Derived Extracellular Vesicles Under Serum-/Xeno-Free Conditions in a Microcarrier-Based Bioreactor Culture System. *Front Cell Dev Biol*. 2020;8(November). doi:10.3389/fcell.2020.553444

48. Lakowicz JR. *Principles of Fluorescence Spectroscopy*. Third Edit. (Springer E, ed.).; 2006. doi:10.1007/978-0-387-46312-4

49. Davenport L, Dale RE, Bisby RH, Cundall RB. Transverse Location of the Fluorescent Probe l,6-Diphenyl-l,3,5-hexatriene in Model Lipid Bilayer Membrane Systems by Resonance Excitation Energy Transfer. *Biochemistry*. 1985;24(15):4097-4108. doi:10.1021/bi00336a044

50. Airoldi C, Mourtas S, Cardona F, et al. Nanoliposomes presenting on surface a cis-glycofused benzopyran compound display binding affinity and aggregation inhibition ability towards Amyloid β1-42 peptide. *Eur J Med Chem*. 2014;85:43-50. doi:10.1016/j.ejmech.2014.07.085

51. Miners JS, Kehoe PG, Love S. Immunocapture-based fluorometric assay for the measurement of insulin-degrading enzyme activity in brain tissue homogenates. *J Neurosci Methods*. 2008;169(1):177-181. doi:10.1016/j.jneumeth.2007.12.003

52. Wang S, Wang R, Chen L, Bennett DA, Dickson DW, Wang DS. Expression and functional profiling of neprilysin, insulin-degrading enzyme, and endothelin-converting enzyme in

prospectively studied elderly and Alzheimer's brain. *J Neurochem*. 2010;115(1):47-57. doi:10.1111/j.1471-4159.2010.06899.x